Morphology, variation, and systematics of the late Cambrian Laurentian dikelocephalid trilobite *Walcottaspis vanhornei* (Walcott, 1914)

Shravya Srivastava* and Nigel C. Hughes

Department of Earth and Planetary Sciences, University of California, Riverside, CA 92521, USA <ssriv008@ucr.edu>, <nigel.hughes@ucr.edu>

Abstract.—*Walcottaspis vanhornei* (Walcott, 1914) is a large, late Cambrian trilobite with a unique pygidial morphology known only from a narrow outcrop belt of the St. Lawrence Formation in the Upper Mississippi Valley. Found in carbonate-rich layers within heterolithic facies that represent the toesets of a prograding shoreface, it is restricted to a single or small number of parasequences. Only four specimens of any of its sclerites have been illustrated previously. Here holaspid examples of all its biomineralized sclerites are described and illustrated, along with a morphometric analysis of cranidial landmarks and landmarks plus semilandmarks for the pygidium. Ontogenetic allometry accounts for 29% of the variance among holaspid cranidia and includes a relative shortening and narrowing of the palpebral lobe and a reduction in the relative length and width of the frontal area. Notable pygidial phenotypic variation occurs in the extent of the postaxial region and in the proportion of the structure occupied by the axis. Phylogenetic analysis suggests that *W. vanhornei* is sister taxon to *Dikelocephalus minnesotensis* Owen, 1852, which also occurs in the St. Lawrence Formation and has a broadly similar cephalon but distinctive trunk. The holaspid pygidium of *W. vanhornei* is uniquely characterized by the interpleural furrows of the first two segments becoming abruptly obsolete on approaching the axial furrow. Some pygidia show narrow, shallow, flat-bottomed grooves etched into the internal sides of the dorsal surface or doublure that apparently represent infestation of the live trilobite.

Introduction

Walcottaspis vanhornei (Walcott, 1914) is a large but little-known dikelocephalid trilobite confined to a narrow outcrop belt of the St. Lawrence Formation in the Upper Mississippi Valley. Only four examples of any of its sclerites have previously been illustrated (Walcott, 1914, pl. 62, figs. 1–3; Ulrich and Resser, 1930, pl. 20, figs. 3–5). This paper describes its morphology, ontogeny, and systematics and considers aspects of its paleoecology. It complements a forthcoming study of evolutionary patterns among dikelocephalid trilobites from this region. Study of this group is potentially instructive from an evolutionary perspective because the region contains a thin but relatively complete (Runkel, 1994; Runkel et al., 2007) record of late Cambrian depositional history formed close to the paleoshoreline. During that time, a condensed suite of nearshore facies was deposited in the Hollandale embayment (Mossler, 1992) within the northern part of the Mississippi Valley. The Hollandale embayment reflects an ancient rift basin located between the Wisconsin arch to the east and the putative "Transcontinental Arch" (Myrow et al., 2003) to the west, two regions of positive relief that were reportedly intermittently exposed during the late Cambrian. This onshore environmental setting, comparable in some ways to modern coastal environments, may have offered opportunity for localized habitat fragmentation and thus enhanced opportunity for speciation, as seen among living marine organisms (e.g., Shen et al., 2011; Dolby et al., 2018). Paleontological evidence suggests that nearshore marine sites were commonly those in which novel morphologies or ecologies first appeared (e.g., Jablonski et al., 1983; Jablonski and Bottjer, 1990; Sepkoski, 1991; Jacobs and Lindberg, 1998). Given this, detailed studies of morphological and ecological evolution in ancient nearshore sites have particular currency but are challenging because such environments are generally poorly preserved. The late Cambrian of the Upper Mississippi Valley provides an important and potentially instructive exception.

Geological setting

Localities.—Specimens of *Walcottaspis vanhornei* are known from at least three localities (Fig. 1) from which most were obtained over one hundred years ago. One of these sites, Hokah (HH), was recollected by the late Gerald O. Gunderson and N.C.H in recent years. It is located at the intersection of Carlson Road and Hwy 16, ∼ 4 km west of Hokah, Houston County, Minnesota (43°46′0.12″N, 91°25′26.4″W) and is apparently the site previously recorded as "Whiteman's Quarry on Mt Hope," USGS Locality #346d (Hughes, 1993, p. 25). Previous records also mention another site at Hokah yielding *W. vanhornei* to be "near old railroad embankment" or "Rail Road Dam," but this is unlikely to have been the HH

CrossMark
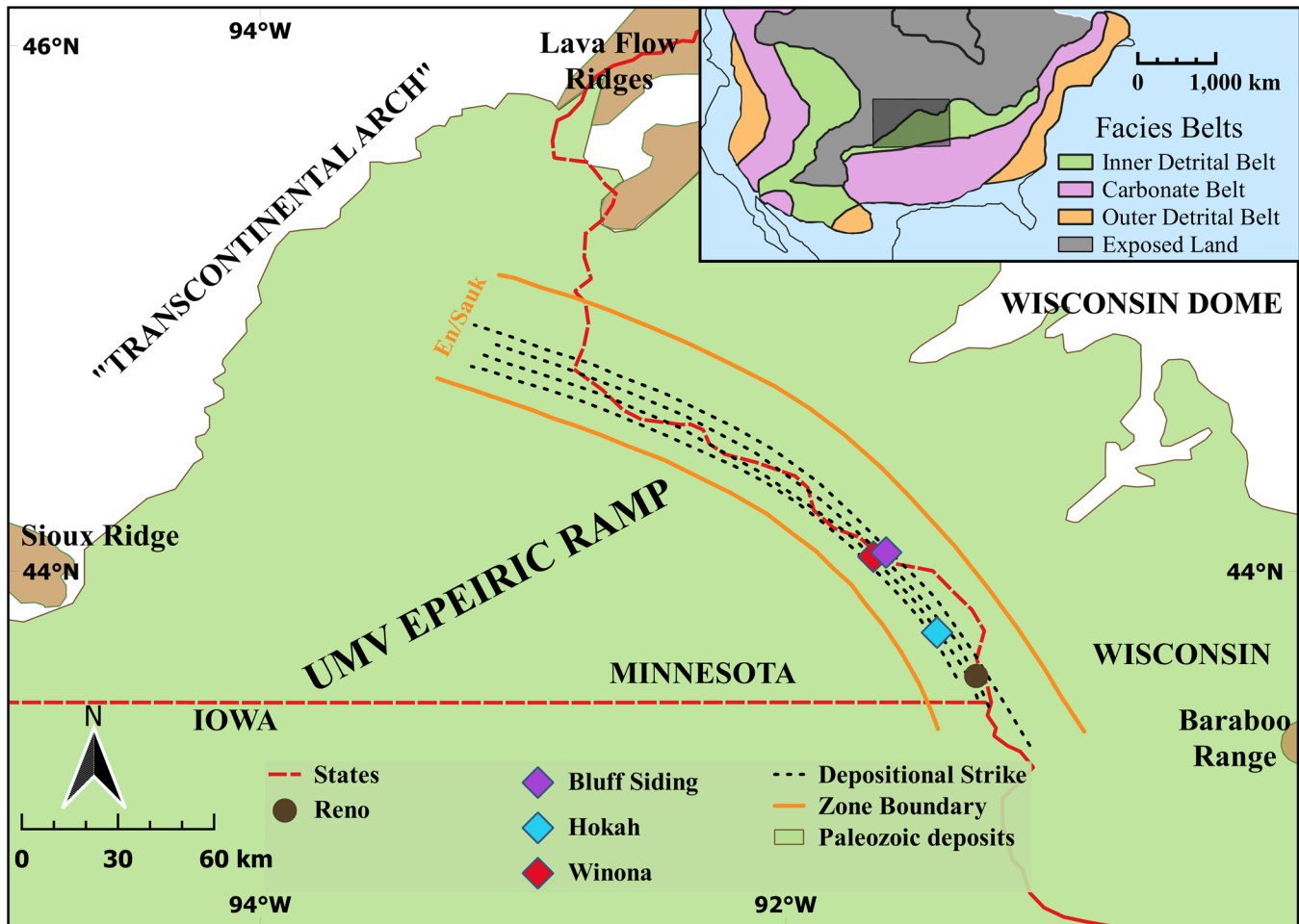
Figure 1.   Location of Upper Mississippi Valley (UMV) region of the North American cratonic interior showing where lower Paleozoic strata are present. Localities yielding *Walcottaspis vanhornei* are shown with diamond-shaped symbols (i.e., Bluff Siding, Wisconsin; Winona and Hokah, Minnesota). Reno, Minnesota, is shown with a brown circle. Inset shows the location of UMV region (shaded area) with respect to the late Cambrian continental lithofacies belts of Palmer (1960). Depositional strike lines are based on Runkel et al. (2007), and *Eoconodontus notchpeakensis–Saukiella* (En/Sauk) subzone boundary is based on Bell et al. (1956), Nelson (1956), and Miller et al. (2003).

site because that is at the top of a notable bluff, as are all outcrops of the St. Lawrence Formation in this area.

The specific positions of two other sites that have yielded reposited *W. vanhornei* specimens are unknown, but given the density of settlement in the area at the time they were collected, both localities will have been at most within a few kilometers of the places named. The Winona (WI; see Hughes, 1993), Winona County, Minnesota, site was reported as on the bluffs facing the Mississippi River, immediately west of the town and in the general vicinity of 44°3′N, 91°43′W (Walcott, 1914, p. 373). Bluff Sliding is in Buffalo County, Wisconsin, and lies on the eastern bank of the Mississippi River immediately opposite Winona. The St. Lawrence Formation crops out in the bluffs above the settlement, for example, in an overgrown roadcut at 44°5′8.82″N, 91°37′15.12″W, but the specific locality from which the specimens were collected is also unknown. The only other reported occurrences of *W. vanhornei* known to us are that of Raasch (1951, p. 142), who reported that Charles Bell and Robert Berg made a find near Reno, Minnesota, and Ulrich and Resser's (1930, p. 66) report of "an imperfect cranidium" from Lodi, Wisconsin. No specimens from near Reno are

available, but the settlement at Reno accords with an arc of outcrop defined by the other three localities and the Runkel et al. (2007) prograding shoreface model (Fig. 1), and we consider this report to be credible. Although to our knowledge we have not seen the Lodi specimen to which Ulrich and Resser (1930) referred, occurrence of genuine *W. vanhornei* at Lodi is unlikely given its geographical position (and stratigraphic position as inferred from Runkel et al., 2007) and, as *Walcottaspis* cranidia strongly resemble those of *D. minnesotensis* Owen, 1852, we consider this reported occurrence to be unsubstantiated.

Taphonomy.—Sclerites of *W. vanhornei* became disarticulated, apparently completely, before recovery and are somewhat flattened/fractured composite molds. They occur in dolomitic siltstone layers within the heterolithic facies of the St. Lawrence Formation (Fig. 2) and are preserved in a manner similar to many examples of their close relative *D. minnesotensis* (see the following and Hughes, 1993). The *W. vanhornei* we have collected lie parallel to bedding (Figs. 3–6), and this appears to be their general condition (in contrast to some beds rich in *Dikelocephalus,* in which specimens may be inclined). The
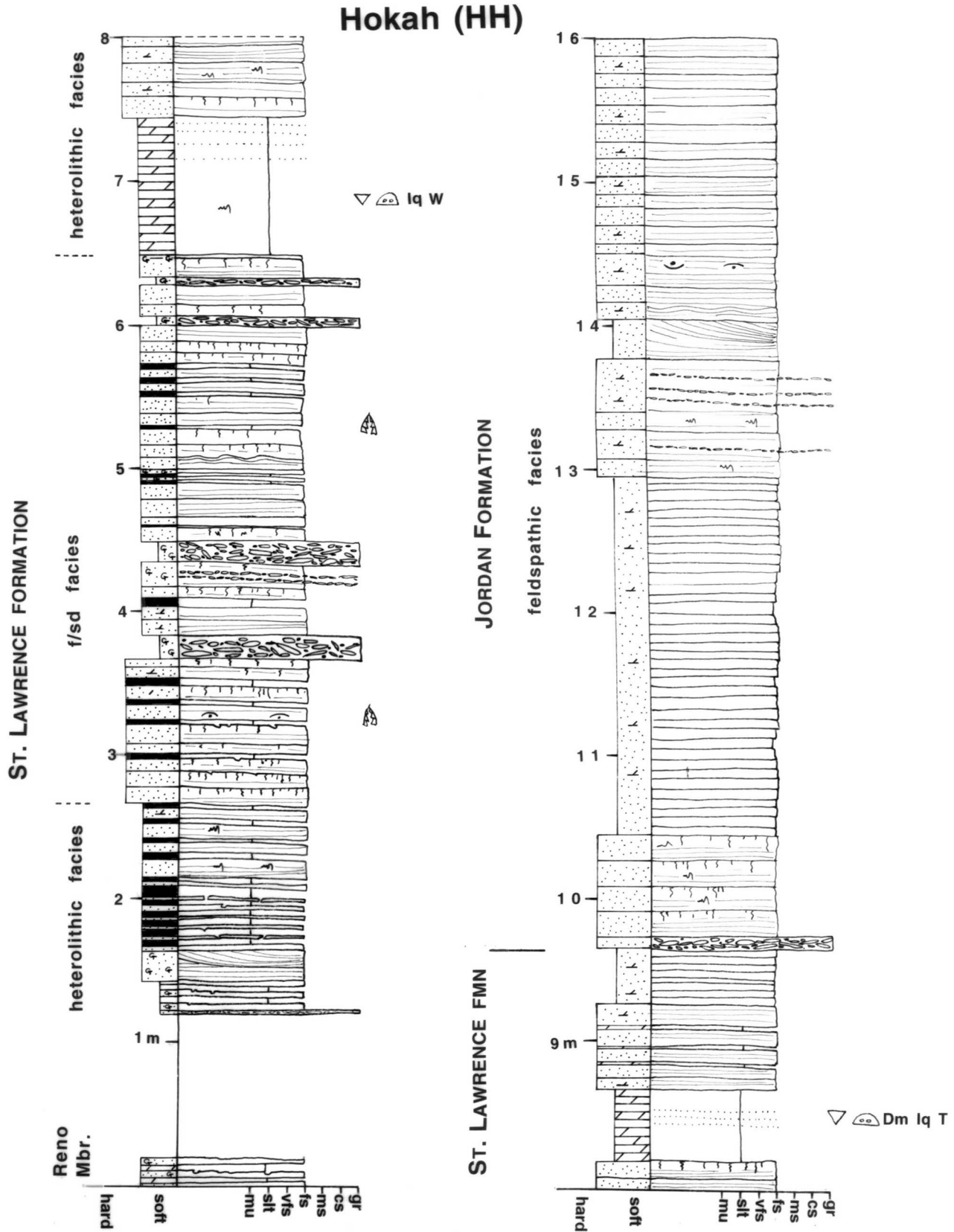
Figure 2. Stratigraphic section of St. Lawrence Formation and adjacent units at locality Hokah (HH), Houston County, Minnesota. Left column depicts lithology and degree of induration with glauconite (G) and mudstone (black). Symbols on the right side of the log refer to the presence of dendroid graptolites (tuning-fork-like symbol), inarticulate brachiopods ('V'), and aglaspidids (half-moon-like symbol). The trilobite occurrences marked on the log include: *Illaenurus quadratus* (Iq), *Dikelocephalus minnesotensis* (Dm), *Walcottaspis vanhornei* (W), *Tellerina* (T). Mbr = member; Fmn = formation; f/sd facies = feldspathic facies. See Hughes and Hesselbo (1997) for further details.

preservation of conjoined free cheeks along with apparently intact genal spines (Figs. 4.10, 4.11, 6.1) argues against significant reworking at the sediment–water interface. Early ontogenetic stages are missing, perhaps because their sclerites were insufficiently robust to be preserved in this environment or juvenile growth was spatially localized elsewhere (e.g., Beheregaray and Sunnucks, 2001). Specimens may have derived from assemblages of individuals alive penecontemporaneously, or from post-exuvial trilobite assemblages, followed by some degree of amalgamation among temporally successive assemblages (Olszewski, 1999). Thus, the "paleontological resolution" (Kowalewski and Bambach, 2003), the span of time represented between those individuals alive most recently and those alive longest ago, is likely to have been no longer than years to decades at most. It may be that some beds exclusively represent exuviae and/or carcasses of contemporary individuals that have since been only slightly reworked taphonomically. Thus, these assemblages may offer a glimpse of the ambient local seafloor situation at high temporal resolution, as is increasingly being recognized among such deposits (e.g., Paola et al., 2018).

Westrop (1986, p. 29) considered the effect of compaction on the cranidial morphology of *Walcottaspis*, then known only from one illustrated specimen, and suggested that Lochman's (in Harrington et al., 1959, p. 254–255) diagnosis of its low relief may reflect sediment compaction. Specimens of both *D. minnesotensis* and *W. vanhornei* from the heterolithic facies show similar patterns of flattening and compression-related cracking, with larger specimens such as FMNH-UC14393a (Fig. 3.11) showing an overall greater degree of cracking than smaller ones, as is typical among trilobites (Hughes, 1999). However, differences in the cranidial morphologies of these species cannot be assigned primarily to taphonomic effects. While all *W. vanhornei* cranidia show effaced S1 and S2 furrows, several such specimens preserve steep-sided, markedly inflated glabellae that have not suffered significant compaction (Fig. 3.1, 3.3, 3.6, 3.9). Accordingly, effacement of the glabellar furrows was an original biological feature and serves to distinguish *Walcottaspis* cranidia from those of *D. minnesotensis,* in which these furrows are notably incised.

As is also common in *D. minnesotensis* (see Hughes, 1993, p. 15), infestation resulted in shallow, flat-bottomed grooves etched into the interior surfaces of both the dorsal surface and the doublure of *W. vanhornei*. As the specimens are preserved as composite molds, these original grooves can also appear as ridges when cast on the underside of the dorsal exoskeleton. The organism responsible was presumably exploiting the interface between the internal surface of the exoskeleton and the soft tissues immediately adjacent. Grooves on the interiors of the dorsal and ventral surfaces are between 0.48 and 0.80 mm wide and do not mirror each other, suggesting independent origin on each surface. As in *D. minnesotensis,* these structures are particularly evident in the pygidium (Fig. 5.2, 5.3, 5.4, 5.7), where they, although sinuous or with angular junctions, tend to extend between the axis (where their author presumably gained entrance) and the lateral margin. A possibly similar groove occurs in a free cheek (Fig. 4.10). These structures were likely the result of either a metazoan parasite or a scavenger that was mining associated soft tissues and that partially eroded

the exoskeleton as it did so. The similar morphologies and width ranges of these trails in both *W. vanhornei* and *D. minnesotensis* suggest the action of a similar author in each and may be evidence of a shared infester.

Sedimentology.—The St. Lawrence Formation is a fine-grained mixed carbonate mud–sandstone unit comprising three lithofacies that include rare stromatolitic dolomite, a laminated feldspathic sandstone facies containing notable flat pebble conglomerates, and a heterolithic facies in which very fine-grained feldspathic sandstone layers are interbedded with dolomitic mudstones (Hughes and Hesselbo, 1997). All *W. vanhornei* specimens yet recovered are preserved in dolomitic mudstone layers of the heterolithic facies. At Hokah, specimens were collected toward the top of the St. Lawrence Formation from a 0.95 m thick buff-colored dolomitic siltstone bedset located about 6.4 m above the base of the section (Fig. 2). *Walcottaspis vanhornei* specimens are concentrated in a level about 15 cm above the base of this layer. A similar ∼0.5 m dolomitic siltstone containing *D. minnesotensis*, but apparently no *W. vanhornei*, occurs about one meter above this level, with its base at about 8.2 m in the log (Figs. 2, 7).

Co-occurrent fossils and biostratigraphy.—Both the Hokah bedsets containing the large species *D. minnesotensis* and *W. vanhornei* also yielded disarticulated sclerites of the trilobite *Illaenurus quadratus* Hall, 1863 and linguiliform brachiopods. The aglaspidid *Cyclopites vulgaris* Raasch, 1939 co-occurs with *W. vanhornei*, and specimens belonging to the trilobite genus *Tellerina* occur along with *D. minnesotensis* (Fig. 7) in the upper layer, along with fragmentary aglaspidid remains (Fig. 2).

Raasch (1951, p. 148) suggested that *W. vanhornei* defines a distinct biostratigraphic level, the eleventh within his *Saukia* Zone. This interpretation places *W. vanhornei* as a stratigraphically late form in the area and is supported by recent sequence stratigraphic analysis. More recent work suggests that *W. vanhornei* was represented within a local, informally defined *Saukiella* trilobite subzone (Runkel et al., 2007, figs. 5, 6) that lies within the *Eoconodontus* conodont Zone and contains among the youngest St. Lawrence Formation rocks outcropping in the area. The appearance of *Eoconodontus notchpeakensis* Miller, 1969 defines the first subzone of the *Eoconodontus* Zone. This species has been found to the east of Hokah but also in sites farther to the west but has not been recovered as yet from the Hokah section. The *W. vanhornei*-bearing bed at Hokah almost certainly lies within the *Eoconodontus* Zone, but it is not yet clear whether it is within the *Eoconodontus notchpeakensis* subzone or the overlying *Cambrooistodus minutus* subzone, the eponymous species of the latter being a form largely restricted to strongly carbonate-rich facies (A.C. Runkel, personal communication, 2022). *Walcottaspis vanhornei* thus occurs within the younger strata of the St. Lawrence Formation, but not the youngest yet known, which occur farther to the southwest.

Sequence stratigraphic setting.—The heterolithic facies of the St. Lawrence Formation represents the toesets of progradational parasequences deposited early during the
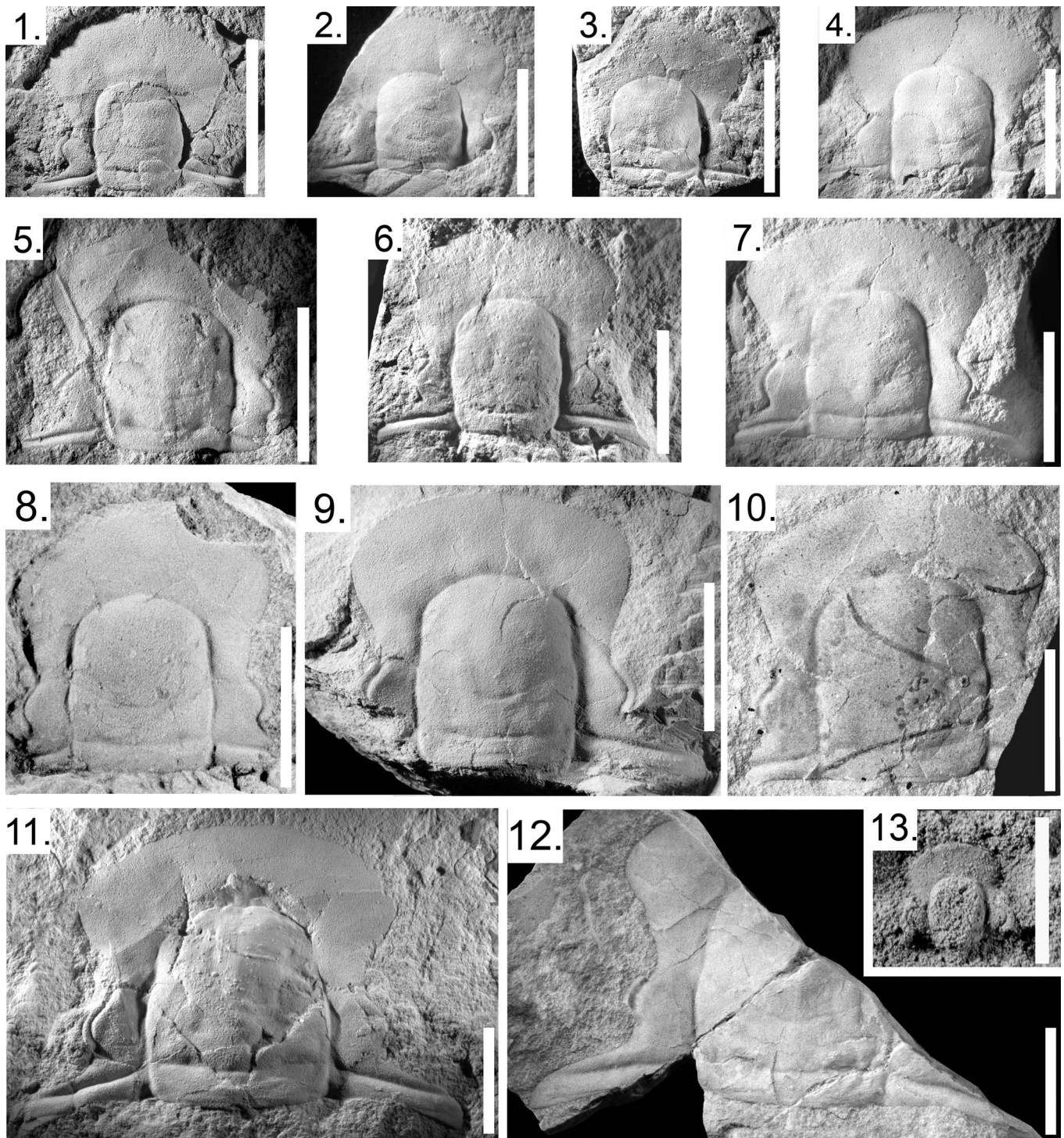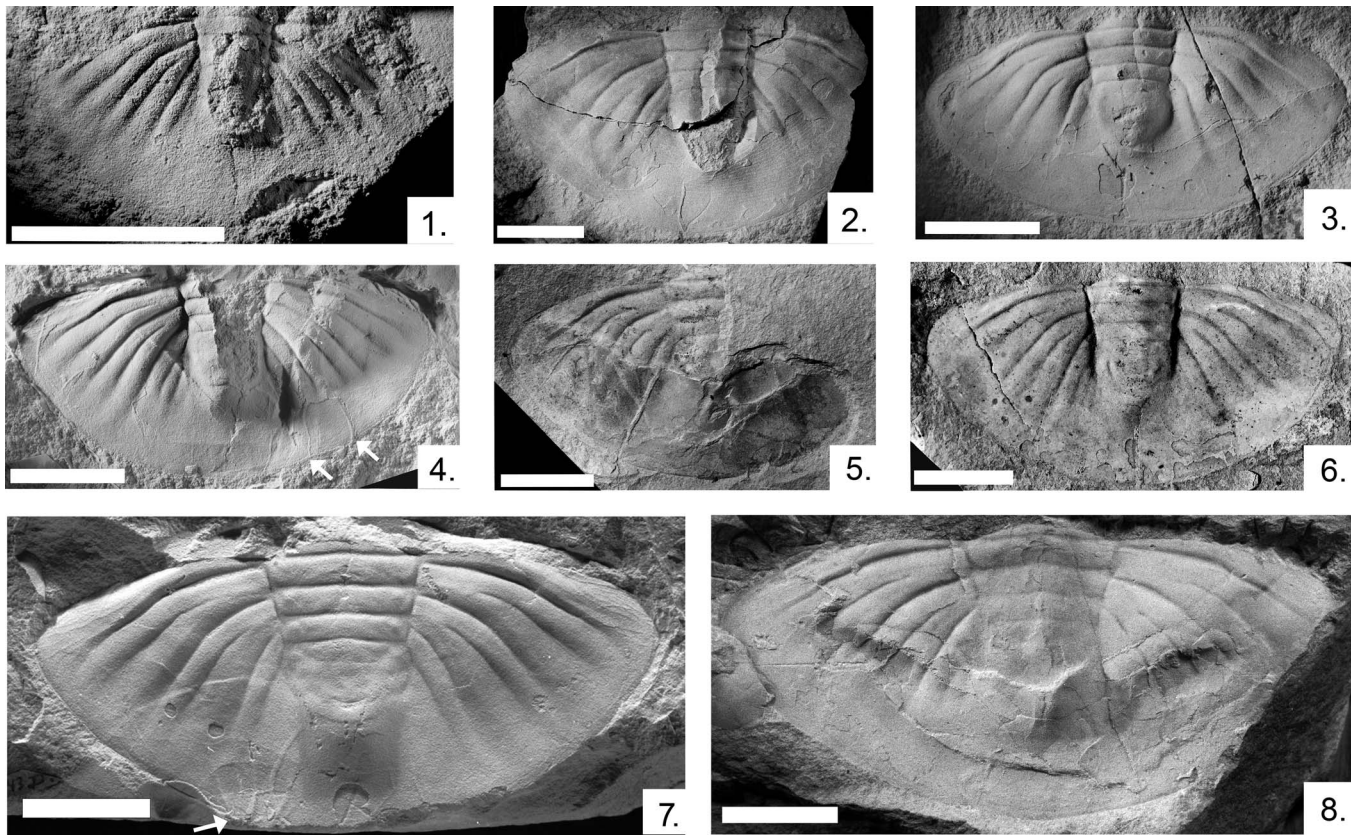
Figure 3. (**1–12**) *Walcottaspis vanhornei* (Walcott, 1914) cranidia from the heterolithic facies of the St. Lawrence Formation at Hokah, Minnesota, in the Upper Mississippi Valley: (**1**) FMNH-UC23314c; (**2**) FMNH-PE39215; (**3**) FMNH-PE39214; (**4**) CMC-IP-89411i (formerly UMPC2443i); (**5**) CMC-IP-87565j (formerly UMPC2443j); (**6**) FMNH-UC23314a; (**7**) CMC-IP-89411h (formerly UMPC2443h); (**8**) CMC-IP-87565x (formerly UMPC2443x); (**9**) CMC-IP-95630 (formerly UMPC3689); (**10**) UWGM 7151 (formerly UW4006-491); (**11**) FMNH-UC14393a, paralectotype; (**12**) CMC-IP-87565t (formerly UMPC2443t). (**13**) Small holaspid cranidium, likely *Dikelocephalus,* from Trempealeau, Wisconsin, holotype of *D. juvenalis* Ulrich and Resser, 1930, USNM-PAL-58601. (**1–12**) Scale bars = 20 mm; (**13**) scale bar = 10 mm.

deposition of a falling-stage systems tract (Runkel et al., 2007) at ca. 490 Ma. Although recognizing individual parasequences within the St. Lawrence Formation can be challenging (perhaps because these deposits represent the toesets of the prograding shoreline where depositional and preservational events were relatively rare and haphazard), the beds containing *W. vanhornei* and *D. minnesotensis* at Hokah evidently belong to different parasequences and are separated by seven ~10 cm
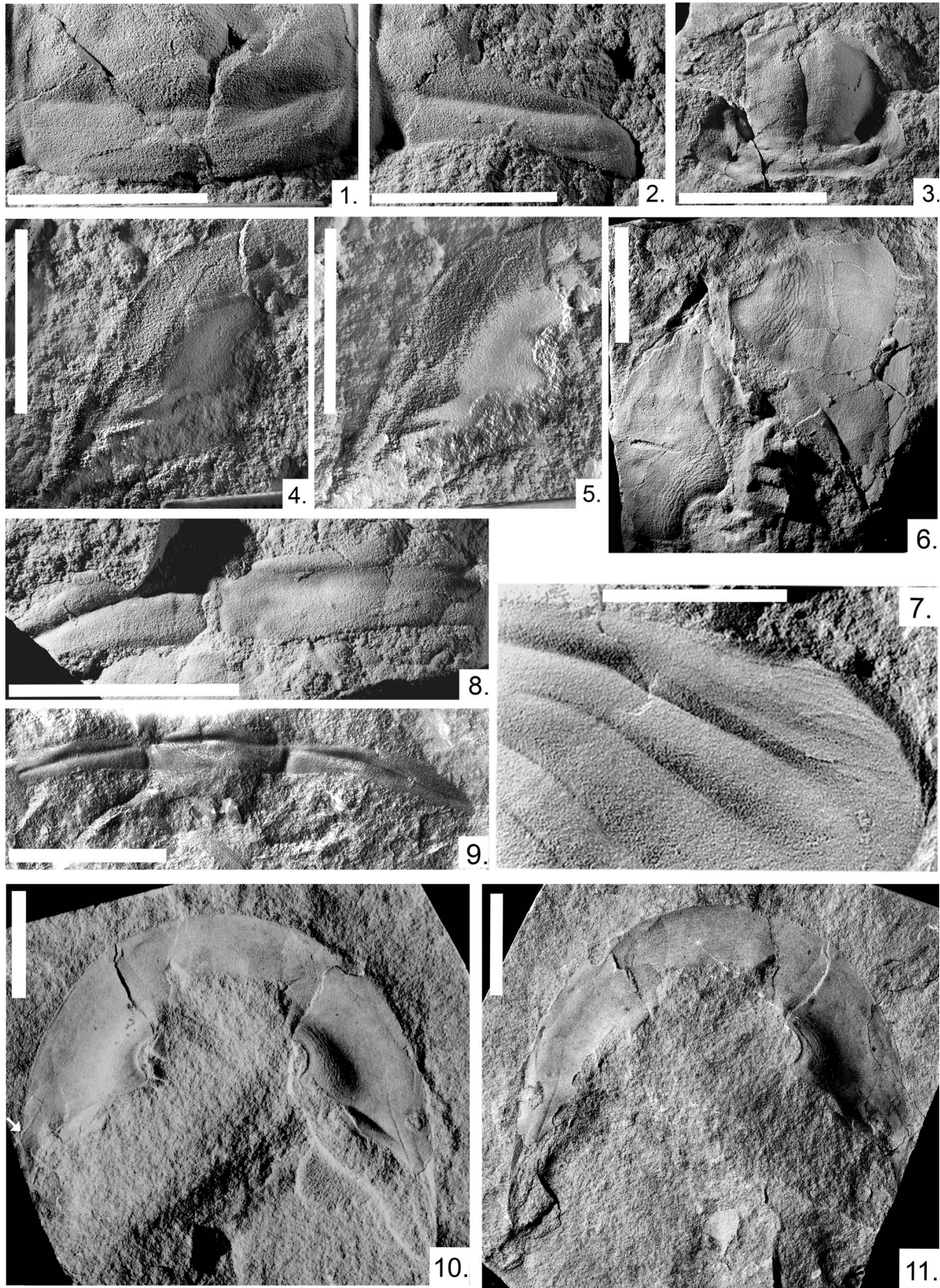
Figure 4. (**1–9**) *Walcottaspis vanhornei* (Walcott, 1914) sclerites from the heterolithic facies of the St. Lawrence Formation at Hokah, Minnesota in the Upper Mississippi Valley: (**1**) detail of glabella of FMNH-UC14393a, paralectotype; (**2**) detail of posterolateral border, FMNH-UC14393a, paralectotype; (**3**) hypostome, FMNH-UC23314f; (**4**) counterpart of right librigena, FMNH-PE82161; (**5**) pixel inversion of (**4**); (**6**) two right librigena on same slab, FMNH-UC23314h; (**7**) detail of FMNH-UC14393b showing terrace ridges, lectotype; (**8**) axial part of thoracic segment, FMNH-PE82162. (**9**) Pixel inversion of counterpart thoracic segment, FMNH-UC14393c, paralectotype. (**10**) Conjoined free cheek from Bluff Siding, Wisconsin, MCZ-IP917 (arrow points to an example of a sinuous structure interpreted to reflect infestation); (**11**) counterpart of conjoined free cheek from Bluff Siding, Wisconsin, MCZ-IP917. Scale bars = 20 mm.

Figure 5. (**1–3, 5, 7, 8**) *Walcottaspis vanhornei* (Walcott, 1914) pygidia from the heterolithic facies of the St. Lawrence Formation at Hokah, Minnesota, in the Upper Mississippi Valley: (**1**) FMNH-PE39210; (**2**) CMC–IP 97568 (formerly UMPC6352); (**3**) CMC-IP 89411c (formerly UMPC2443c). (**4**) From Winona, Minnesota, USNM-PAL 72687A. (**5**) UWGM 7161 (formerly UW4006-501). (**6**) From Bluff Siding, Wisconsin, MCZ-IP910. (**7**) FMNH-UC14393b, lectotype; (**8**) CMC-IP 89411a (formerly UMPC2443a). Scale bars = 20 mm. Arrows in (**4, 7**) point to examples of sinuous structures interpreted to reflect infestation.

thick beds of parallel laminated feldspathic sandstone with burrowed tops, which may each represent deposition from a notable storm (Fig. 2).

During deposition of the highstand and falling-stage systems tracts, the shoreline in the Upper Mississippi Valley prograded basinward (i.e., toward the southwest) (Runkel et al., 2007). As the rate of relative sea-level rise declined, sediment supply from the land exceeded the generation of accommodation space, leading to deposition of regressive facies and the outward migration of the shoreface. The result was a series of parasequences whose lateral facies coarsened shoreward, the more offshore, distal toesets of which were characterized by carbonate muds of the heterolithic facies. Their proximal equivalent was fine-grained sandstones characteristic of the Norwalk Member of the Jordan Formation, but similar lithologies frequently also interbed with the finer-grained carbonates within the heterolithic facies of the St. Lawrence Formation, as stated. Such sandstone beds resulted from depositional events of sufficient magnitude to transport land-derived sediment into this part of the basin and, where concentrated, constitute the feldspathic sandstone facies of the St. Lawrence Formation. Flat pebble conglomerates are also common in these facies and, in some cases, indicate episodes of marked stratigraphic condensation (Hughes and Hesselbo, 1997).

The geographical positions of the three verified localities from which known *W. vanhornei* specimens have been recovered fall almost exactly along the projected position of the

prograding shoreline according to Runkel et al. (2007, fig. 1; Fig. 8). In doing so, they provide additional evidence for the validity of this model. This distribution strongly suggests that the temporal range of *W. vanhornei* was notably short, as Raasch's (1951) biostratigraphic scheme anticipated. To date, *W. vanhornei* has been localized to only a single parasequence at Hokah, and its distribution among localities does not exclude the possibility of occurrence within a single parasequence throughout the region (Fig. 8). This is a minimum, but given the narrow outcrop belt of its occurrence, *W. vanhornei* is unlikely to have been represented at the abundance seen in the bed at Hokah in more than a small number of parasequences, with five being a maximum estimate. On the basis of an estimate of the rate of deposition of the entire Croixan Series, Runkel et al. (2007, fig. 11) suggested the average duration of a parasequence within the basin to range between 75,000 and 150,000 years. However, during the early falling-stage systems tract, parasequence duration was likely to have been at the short end of this range and perhaps closer to 50,000 years (A.C. Runkel, personal communication, 2021). The duration of the known fossil record of *W. vanhornei* thus likely represents an interval not much greater than about 250,000 years, and likely substantially shorter.

Although we have yet to recover trilobites within the St. Lawrence Formation at Hokah below the layer containing *W. vanhornei* (Fig. 2), regional relationships show that *D. minnesotensis* occurred widely throughout the region in
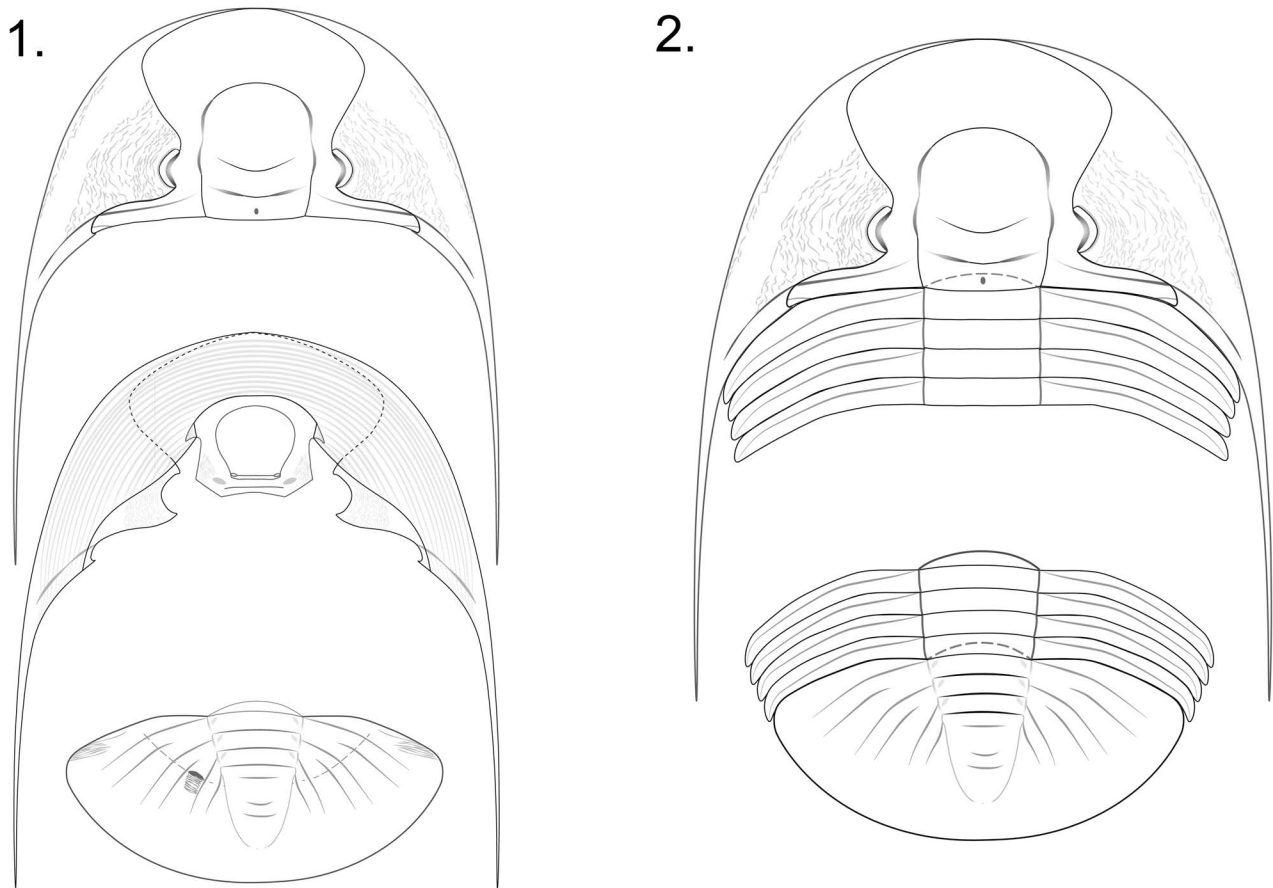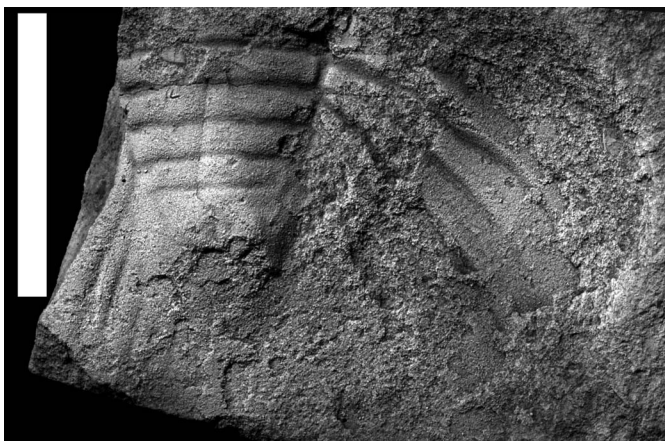
Figure 6. Reconstruction of holaspid *Walcottaspis vanhornei*. (**1**) Dorsal view of cranidium with median tubercle, free cheek with eye platform, and surface ornamentation; ventral view of conjoined free cheek with terrace ridges and hypostome with surface ornamentation; and dorsal view of pygidium showing petaloid facet, paradoublural line (dashed), and terrace ridges on the dorsal surface of the venter ventral side of pygidium. (**2**) Dorsal view of holaspid with estimated trunk proportions. The relative sizes of the cephalon and pygidium are drawn such that, upon putative enrollment, their marginal outlines match optimally in shape (see text for details).

both the heterolithic and feldspathic sandstone facies, including in areas where St. Lawrence Formation deposition predated that recorded at Hokah. The occurrence of *D. minnesotensis* both in

Figure 7. *Dikelocephalus minnesotensis* pygidium (UWGM7065) recovered from a dolomitic siltstone bed, the base of which is at about 8.2 m in the Hokah (HH) outcrop section, approximately one meter above the level containing the *Walcottaspis vanhornei* specimens collected in this study. This helps demonstrate that *W. vanhornei* occurs within the temporal range of *D. minnesotensis*. Scale bar = 20 mm.

the next fossil-bearing bed above those containing *W. vanhornei* (Figs. 2, 7) and at localities farther west, such as Rushford, Minnesota, confirms Raasch's (1951) view that the range of *W. vanhornei* occupied only a small portion of the regional temporal range of *D. minnesotensis* and that *D. minnesotensis* evidently regained its local abundance in the heterolithic facies shortly after a time in which *W. vanhornei* apparently had sole local representation.
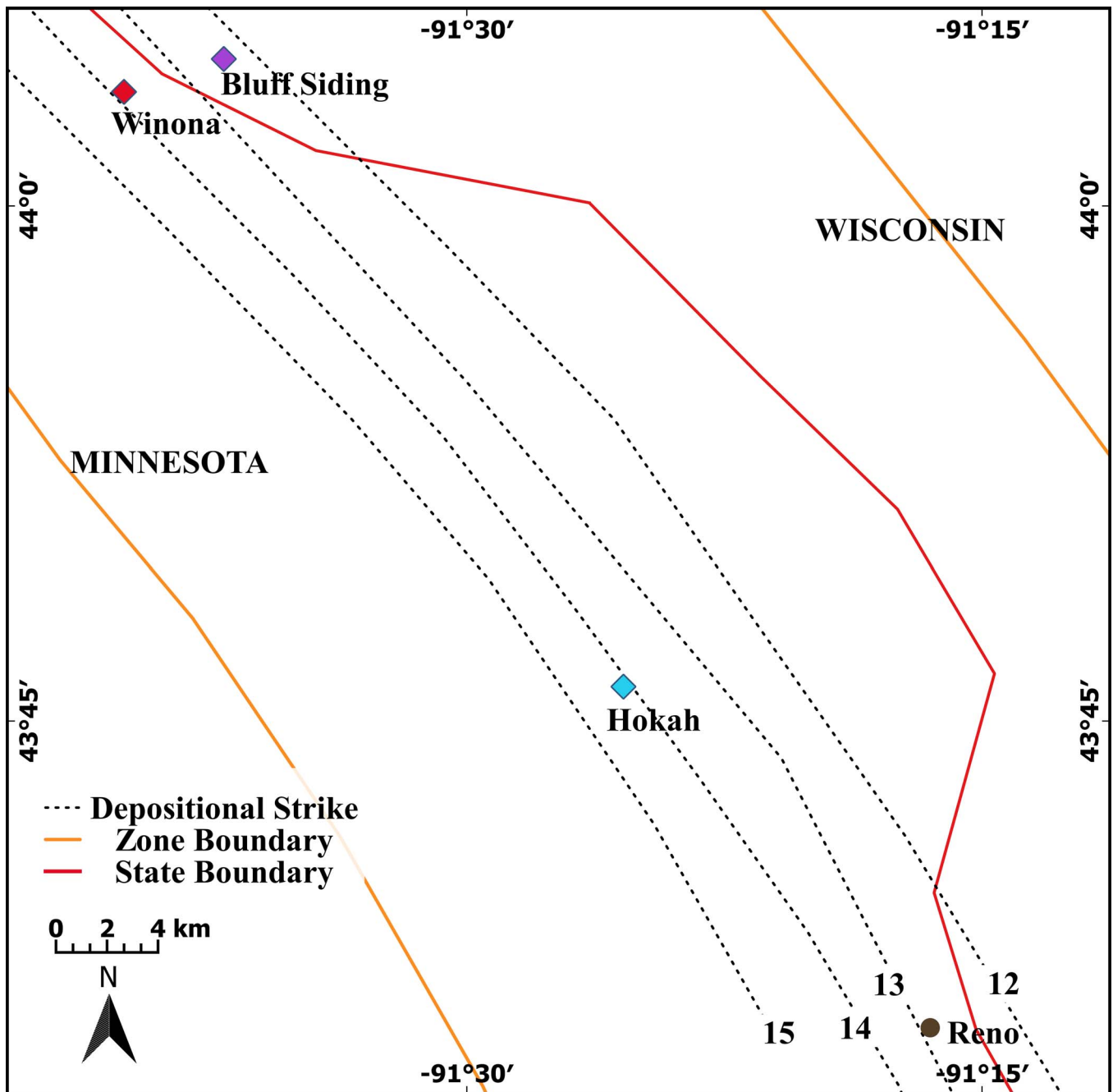
Published views on *Walcottaspis vanhornei* morphology and systematic affinities

Dikelocephalus vanhornei was introduced by Walcott (1914, p. 373), who illustrated and described one counterpart cranidium, one thoracic segment, and one pygidium. He noted that although its cranidium was closely similar to that of the comparably large trilobite *D. minnesotensis*, its pygidium was strikingly different. The genus *Walcottaspis* was established by Ulrich and Resser (1930, p. 66–68), who refigured Walcott's part cranidium and pygidium, along with the illustration of one additional pygidium. Their justification for generic status was the markedly distinct pygidial structure including the termination of the pleural furrow abaxially to the axial furrow, the one fewer clearly defined axial segment, the absence of marginal spines, the

Figure 8. Spatial distribution of *Walcottaspis vanhornei* in the four localities from Figure 1, consistent with occurrence possibly restricted to the geographical range of a single parasequence of the En/Sauk subzone as defined by Runkel et al. (2007).

transverse anterior pygidial margin, and its elliptical posterior margin. With respect to closest relatives, Walcott (1914) compared *W. vanhornei* only with *D. minnesotensis*, but Ulrich and Resser (1930, p. 64) placed it with species of the genus *Osceolia,* also known only from the Upper Mississippi Valley, in their newly defined subfamily Osceolinae, from which *Dikelocephalus* was excluded. The basis for this grouping was that the pygidial interpleural furrows of *Walcottaspis* and *Osceolia* are partly or wholly obsolete and that the members of both genera have only four clearly defined pygidial axial rings, rather than the five that they considered characteristic of *Dikelocephalus* (Ulrich and Resser, 1930, p. 65–66). They further supported

this assertion by reference to unpublished specimens suggested to be allied to *Osceolia* from the "Devil's Lake Sandstone," a nearshore facies variant of the Reno Member of the Tunnel City Group but which lack marginal pygidial spines. The name that Ulrich and Resser (1930, p. 68) gave to that material, "*Osceolina diabolo*," is a nomen nudum, the whereabouts of its specimens is unclear, and no further material of this kind has subsequently been reported.

Lochman (1956, fig. 2) suggested that *Walcottaspis* was derived from an unspecified species or species lineage within the genus *Briscoia,* which she considered to be explicitly polyphyletic and derived directly, in her view, from two different
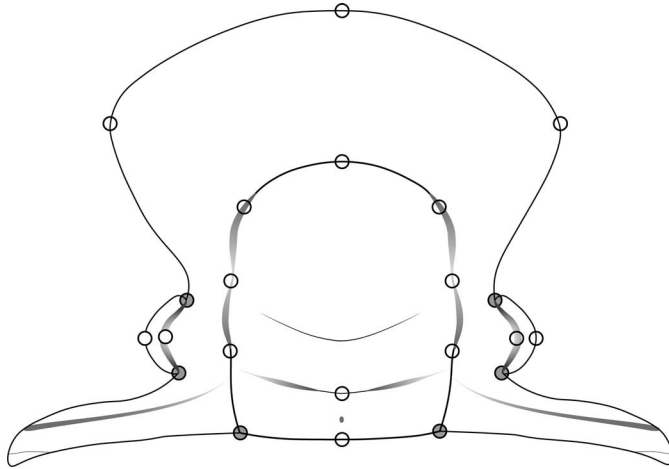
Figure 9. Reconstruction of *Walcottaspis vanhornei* cranidium showing the set of 22 landmarks selected to optimally capture variation among the specimens available. Specimens had to preserve all four axial landmarks and at last one of each of the paired abaxial landmarks to be included in the dataset. Type 1 landmarks (Bookstein, 1991) are shown as gray-shaded circles, Type 2 landmarks as open circles.

species of the idahoiid *Wilbernia* (Fig. 10). She did not provide character-based support for the particular links invoked but wrote of certain "irreversible trends in the evolution of Dikelocephalidae" (Lochman, 1956, p. 449), some of which, such as the squaring of the anterior glabella and the obsolescence of the anterior border furrow, are present in *W. vanhornei*. Others, such as increased eye length and shortened posterolateral border relative to putative ancestors, are not. Given Lochman's (1956) recognition of explicitly polyphyletic genera without specification of putative phylogenetically informative characters within these, the reasoning for her association of *W. vanhornei* with a species within *Briscoia* is unclear, as is that justifying her derivation of *Osceolia* and two branches of a polyphyletic *Dikelocephalus* from other unspecified *Briscoia* species.

Westrop's (1986, p. 29) consideration of the effect of compaction (see the preceding) compared *W. vanhornei* directly with St. Lawrence Formation *Dikelocephalus,* and no other taxa.

A report of two cranidia assigned to *Walcottaspis* sp. from substantially older Cambrian rocks in the Himalaya (Shah et al., 1991, p. 91, pl. 1j, n) was based on misidentification. The Himalayan specimens, although effaced, differ in having a trapezoidal glabella, strong eye ridges, and in one case, an anterior border. These authors reported the specimens to be of Guzhangian
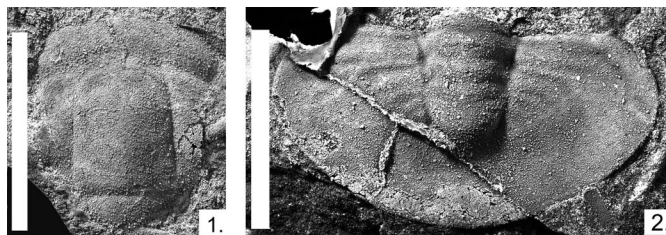
age, some 7.5–6.0 Myr older than *W. vanhornei*, although in our opinion these forms are likely still older. Their features compare better to Wuliuan forms such as *Paramecephalus* (see Zhang et al., 1980, pl. 117, 118, figs. 1–6; Jell and Hughes, 1997, pl. 12; Luo et al., 2009, pl. 13, figs. 3, 4) or *Xingrenaspis dardapurensis* (Jell and Hughes, 1997, pl. 18, figs. 4–11).

Hughes (1994, p. 53) noted that the pygidial axis of *W. vanhornei* displays fewer rings than that of *D. minnesotensis* and suggested that the difference in their morphology might be partly explained if holaspid *D. minnesotensis* retained in its pygidium a segment homologous to the one released into the thorax in holaspid *W. vanhornei*.

Phylogenetic position

Herein we have used primarily parsimony-based phylogenetic analysis, supplemented by a Bayesian maximum likelihood approach, to assess phylogenetic relationships between the various taxa of dikelocephalids bearing an extended cephalic doublure. The cladistic analysis of Dikelocephalidae conducted here uses a branch and bound search of 38 characters divided into a total of 98 character states across 16 ingroup taxa and one outgroup (Table 1; Supplementary Data 1). As some characters varied along a continuous scale, we also conducted a separate parsimony-based analysis treating them as such, rather than with user-imposed, discretized character state divisions as used in the first analysis. Eleven out of a total of 38 characters were continuous and were measured using the most complete sclerites of each species considered (see table in the Supplementary Data 1 for the character states of continuous characters). For both the discretized dataset and the mixed continuous character and discrete character dataset, the outgroup was *Prosaukia misa* (Hall, 1863), chosen for its close similarity with dikelocephalids in having a quadrate glabella and elliptical pygidium but not showing the extended doublure. The species used in the phylogenetic analysis are listed in Supplementary Data 1, with references to their published figures and unpublished images from our image library.

The parsimony analyses were run using Tree Analysis Using New Technology (TNT; Goloboff et al., 2008), and Winclada (Nixon, 2002) was used to map transitions in discrete character states (Fig. 11.1, 11.2) and to calculate support indices (Supplementary Data 2, figs. 1, 2). For the discretized character-state analysis, an implicit enumeration search in TNT resulted in four most parsimonious trees (of which the strict consensus tree is depicted in Fig. 11.1) and a tree length of 141, consistency index of 39, and retention index of 33. Although overall tree resolution is poor, relationships between most well-represented dikelocephalids from the Upper Mississippi Valley are supported by unambiguous synapomorphies and suggest common ancestry among *Dikelocephalus* species and *W. vanhornei,* with *W. vanhornei* as sister taxon to *D. minnesotensis*. Bootstrap resampling was calculated by the GC method for 1,000 replicates with the implicit enumeration search option (Supplementary Data 2, fig. 1). Bremer support (Bremer, 1988, 1994) was calculated by default TBR branch swapping, setting the suboptimal limit to six steps. Both these metrics suggest that relationships of *W. vanhornei* reported in the preceding receive the strongest support within the analysis. Maximum likelihood analysis of the same dataset using MrBayes yields results consistent

Figure 10. *Wilbernia* sp. from the "Hudson Member" of the Lone Rock Formation in the Upper Mississippi Valley from the Winona (Minnesota)/Fountain City (Wisconsin) region showing notable pygidial homeomorphy with *W. vanhornei*. (**1**) UWGM7069, cranidium. (**2**) UWGM7070, latex of counterpart pygidium. Scale bars = 20 mm.

Table 1. Matrix of character states for selected taxa. See Supplementary Data 1 for a descriptive list of characters, character states, and taxa used in this phylogenetic analysis. Columns correspond to character state designations, and rows contain taxa names.

Taxon	Character and Character State (1–38)
Prosaukia misa (Owen, 1852)	0 0 0 0 0 0 0 0 0 0 0 0 0 0 0 0 0 0 0 0 0 0 0 0 0 0 0 0 0 0 0 0 0 0 0 0 0 0
Prosaukia hartii (Walcott, 1879)	0 0 0 0 0 0 0 0 0 0 1 1 0 0 2 0 1 0 0 ? 0 0 0 0 0 0 0 1 2 0 0 0 1 2 2 0 0 0
Briscoia schucherti Ulrich and Resser, 1930	1 0 0 0 0 2 0 2 1 2 2 1 0 0 0 0 1 0 0 0 0 ? 0 ? 0 0 0 0 0 0 0 0 0 2 2 ? 0 0
Briscoia angustilimba Westrop, 1986	0 0 0 0 0 2 0 1 2 2 1 1 0 0 2 0 1 0 0 ? ? ? ? ? 0 0 0 ? 1 0 0 0 1 1 2 1 0 0
Briscoia sinclairensis Walcott, 1924	1 0 0 0 0 2 0 0 1 2 1 1 0 2 0 1 1 0 0 ? ? ? ? ? 0 0 0 2 1 0 0 0 0 1 2 1 0 0
Briscoia dalyi Walcott, 1914	1 0 0 0 1 0 0 1 1 1 0 0 0 0 0 1 1 0 0 0 0 ? 1 ? 1 0 0 2 1 0 0 0 1 2 2 1 0 0
Briscoia llanoensis Winston and Nicholls, 1967	1 0 1 ? 0 0 2 0 1 2 1 0 1 0 0 1 2 0 0 ? 1 ? ? ? 0 1 0 0 0 0 0 0 0 2 2 0 0 0
Briscoia septentrionalis Kobayashi, 1935	1 0 0 2 0 0 2 2 2 0 1 1 0 0 0 0 0 1 0 ? ? ? ? ? 0 0 0 0 2 0 0 0 ? 2 2 0 0 0
Briscoia pertransversa Lochman, 1956	1 0 0 2 3 0 0 2 2 2 0 0 1 2 0 0 0 0 1 ? 0 ? ? ? 0 0 0 0 0 0 0 0 1 0 0 0 0 0
Briscoia coloradoensis Walcott, 1914	1 0 0 2 2 0 0 1 2 2 2 0 0 1 0 1 0 0 0 ? ? ? ? ? 0 0 0 0 1 0 0 0 0 2 2 0 0 0
Briscoia nevadensis Resser, 1937	1 0 0 0 1 0 2 1 1 2 1 0 1 1 0 0 0 0 0 ? ? ? ? ? 0 0 0 2 2 0 0 0 0 0 2 1 0 0
Dikelocephalus minnesotensis Owen, 1852	1 0 0 2 2 2 1 2 2 0 0 0 0 1 1 0 0 1 0 1 1 0 1 1 0 2 2 1 2 1 0 0 0 1 2 0 0 0
Dikelocephalus freeburgensis Feniak in Bell et al., 1952	2 0 1 ? 3 1 1 2 1 1 1 0 0 0 1 0 2 ? 0 ? 1 1 0 1 0 1 0 2 1 1 2 0 1 2 2 1 1 1
Walcottaspis vanhornei (Walcott, 1914)	2 0 0 1 1 1 0 2 2 0 0 0 0 0 1 0 2 1 0 0 1 0 1 ? 0 0 1 2 0 1 0 0 0 2 2 1 2 0
Osceolia sensu lato	1 0 0 0 1 0 0 1 2 2 0 1 0 0 0 0 1 1 0 1 ? ? 0 ? 0 1 0 0 0 0 2 1 1 2 1 0 0 0
Elkia nasuta Walcott, 1884	1 0 0 2 0 0 2 2 2 2 2 0 1 1 1 0 0 0 0 ? ? ? ? ? 0 0 0 0 3 0 1 0 1 0 2 0 2 0
Hamashania pulchera Kobayashi, 1942	2 0 0 2 0 0 1 1 0 1 1 1 1 0 0 0 0 0 0 ? 0 ? ? ? 1 0 0 0 3 0 1 0 1 0 1 0 0 0

with this parsimony-based analysis (Supplementary Data 6), specifically that *D. freeburgensis* Feniak in Bell et al., 1952 is the sister taxon to a clade bearing *W. vanhornei* and *D. minnesotensis,* and that these relationships have posterior probability support comparable to that of other morphological character-based analyses.

For the combined discrete and continuous character-based analysis, TNT implicit enumeration search resulted in a single tree. The 27 discrete characters from this dataset were mapped onto the most parsimonious tree found by TNT (Fig. 11.2), with tree length of 72, consistency index of 48, and retention index of 50. Overall tree resolution is improved and maintains shared ancestry among *Dikelocephalus* species and *W. vanhornei*, with *W. vanhornei* as sister taxon to *D. minnesotensis*. Again, Bremer support and bootstrap resampling show these relationships to receive relatively high levels of support (Supplementary Data 2, fig. 2). This analysis confirms that these phylogenetic conclusions are not the result of arbitrary character state divisions imposed during the discretization of continuous variables.

The results of both the parsimony-based phylogenetic analysis and of maximum likelihood analyses conducted to date suggest *W. vanhornei* to be sister taxon to *Dikelocephalus minnesotensis*, whose stratigraphic range encompasses that of *W. vanhornei* (Fig. 11) and support Walcott's (1914) original comparison between these taxa. The older *Dikelocephalus* form from the transgressive systems tract in the Reno Member, Tunnel City Group, *Dikelocephalus freeburgensis,* is sister taxon to the clade comprising *D. minnesotensis* and *Walcottaspis vanhornei*. *Osceolia* species lie outside the clade bearing *Dikelocephalus* and *Walcottaspis*, and this result predicts that *Osceolia* or its closest relatives will occur in the stratigraphic record before the appearance of the *Dikelocephalus–Walcottaspis* clade. Neither Ulrich and Resser's (1930) nor Lochman's (1956) proposed relationships of *W. vanhornei* are supported, and *Briscoia* remains either an association of plesiomorphic species with unresolved relationships (Fig. 11.1) or polyphyletic (Fig. 11.2). Most *Briscoia* species are based on small numbers of specimens and occurrences widely scattered across Laurentia. A more extensive phylogenetic analysis of dikelocephalids and their relatives is forthcoming but beyond the scope of this paper.

Ulrich and Resser (1930) justified *Walcottaspis* among dikelocephalids largely on the basis of its phenetically distinctive pygidium (see the preceding), and this opinion has not been challenged by any subsequent worker to date. One implication of our phylogenetic analyses is that, if the genus *Walcottaspis* is maintained, the genus *Dikelocephalus* is paraphyletic (Fig. 11). We note this implied paraphyly but defer further consideration until we complete a comprehensive investigation of dikelocephalid morphometry and systematics.

Shape variation

Although specimens assigned to *Walcottaspis vanhornei* share definitive features, morphological variation is evident among its members. Here we use semilandmark- and landmark-based geometric morphometric analysis to explore such variation. Specimens were imaged in dorsal view with the palpebral lobe surface mounted horizontally and the axial pygidial furrow
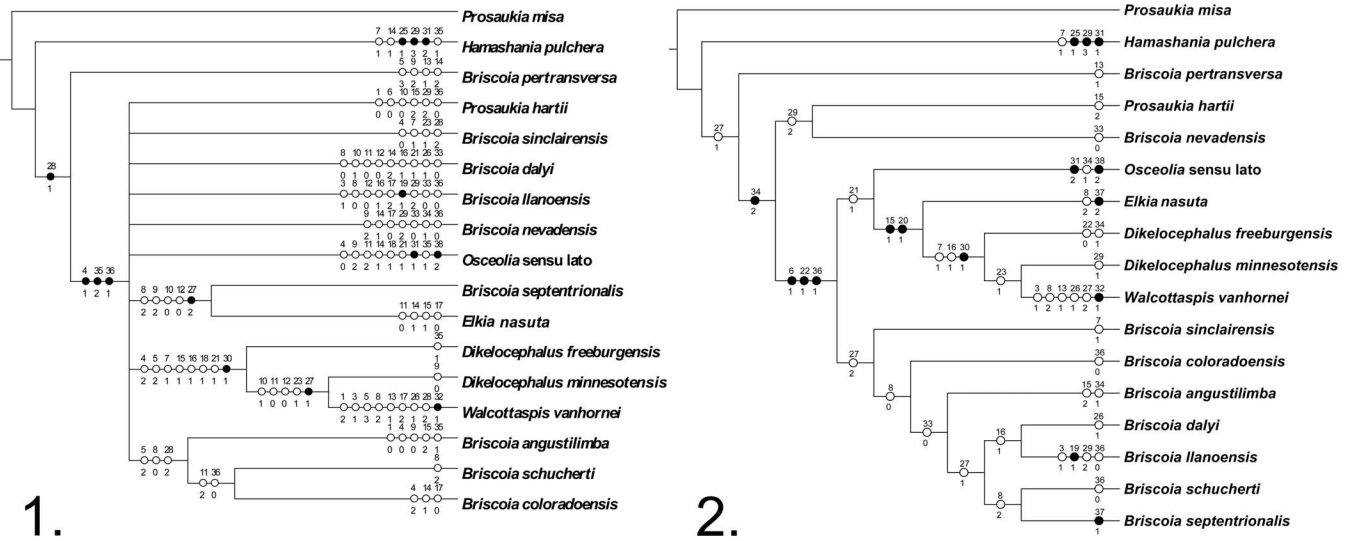
Figure 11. Parsimony-based phylogeny of dikelocephalids using *Prosaukia misa* as the outgroup. (**1**) Strict consensus tree of the four most parsimonious tree found for this character matrix using all characters divided into discretized character states. (**2**) Single tree found for the character matrix using a mixture of discretized and continuous characters. Numbers on top of node branches show the character number, and numbers on bottom show the state for that character. Filled circles indicate unambiguous derived character states while open circles indicate convergent derived character states. Refer to Table 1 for codings, Supplementary Data 1 for list of characters, character states, and selected taxa; refer to Supplementary Data 2 for Bremer support and bootstrap resampling results.
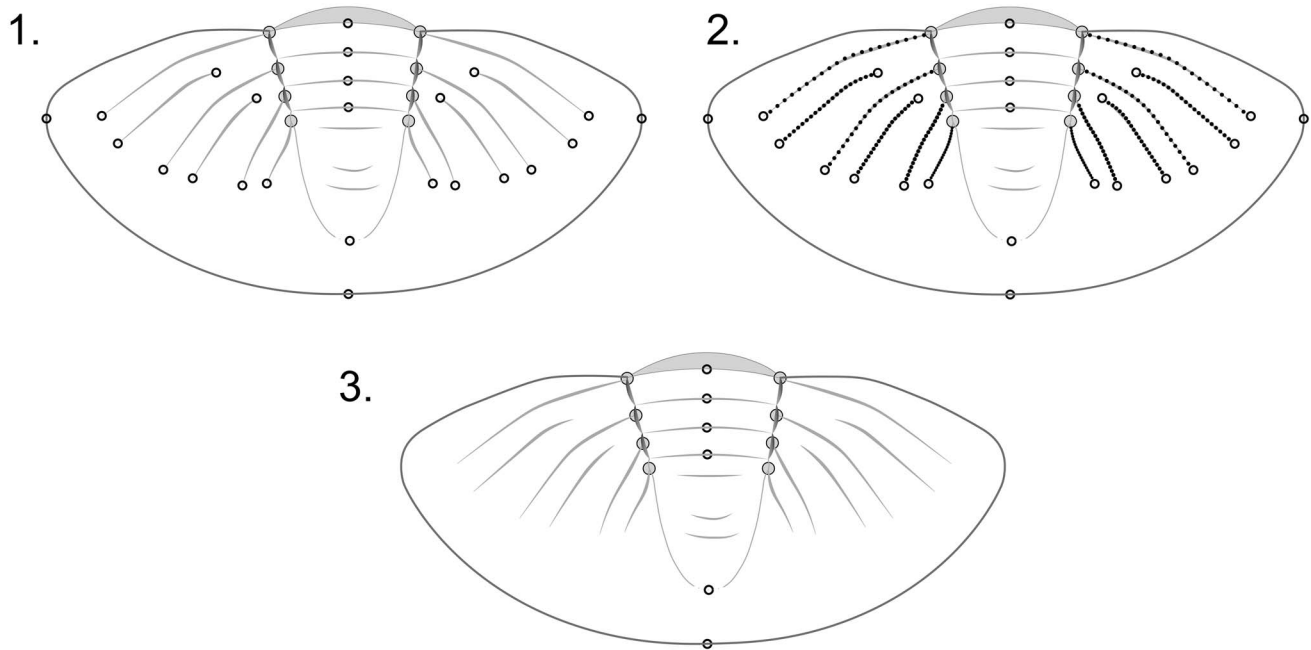
Figure 12. Reconstruction of *Walcottaspis vanhornei* pygidium showing the landmarks used to assess morphological variation in a set of 10 specimens. (**1**) Landmark scheme comprising 40 landmarks capturing features of the axis, the pygidial margin, and extent of pleural and interpleural furrows. (**2**) Landmark scheme of 256 landmarks, including the 40 landmarks mentioned in (**1**) combined with 216 semilandmarks used to trace the positions of the pleural and interpleural furrows. (**3**) Landmark scheme of 14 landmarks capturing only the axial features of the pygidium. Type 1 landmarks are shown as gray-shaded circles, Type 2 landmarks as open circles. Eight additional Type 1 landmarks mark confluence of the pleural and interpleural furrows with the axial furrow. They are not shown in (**1**) and (**2**) because they have near overlap with those landmarks at the intersection of the axial and inter-ring furrows.

mounted horizontally. A set of landmarks were selected: 22 in the cranidium (Fig. 9) and 40 landmarks and 216 semilandmarks in the pygidium, with semilandmarks used to capture information about the pleural and interpleural furrows (Fig. 12.1, 12.2). A pygidial analysis with only the 14 landmarks present on the axial lobe and the axial posterior margin was also

conducted (Fig. 12.3). Except where prohibited, specimens were coated with ammonium chloride sublimate before being photographed. The image library was assembled intermittently between 1986 and 2021 and mostly using a Nikon SRL camera with images captured either as 35 mm black-and-white negatives or directly as digital images. Most were taken within the specimen's host institution. Negatives were digitally scanned with a Polaroid SprintScan 35 plus or an Epson Perfection V700 scanner. Cartesian X and Y coordinates of morphological landmarks for each specimen of cranidia and pygidia were recorded using the freely available software tpsDig (http://www.sbmorphometrics.org/soft-dataacq.html) and ImageJ (https://imagej.nih.gov/ij/download.html). Morphometric analysis of the landmark dataset was conducted using RStudio interface in R (https://www.rstudio.com). In R, the packages used for statistical analysis were geomorph (Adams et al., 2021; Baken et al., 2021) for most of the morphometric functions and prWarp (Mitteroecker et al., 2020; Grunstra et al., 2021) for partial warp analysis. For fitting linear regression models, Residual Randomization Permutation Package (Collyer and Adams, 2018, 2021) was used as it has a high statistical power to identify patterns in data (Anderson and Braak, 2003). Preservation in dolomitic siltstone resulted in specimen compaction, which inflates variance due to taphonomic, as opposed to biological, reasons. While we are confident that such variance does not overwhelm the original biological signal, it conflates it in such a way that we cannot confidently interpret the biological significance of very small differences among specimen shape. Accordingly, rather than some of the more sophisticated estimates of measurement error used in recent analyses (see Hughes et al., 2021), we used a simple estimate of measurement error involving multiple remounting, reimaging, and redigitizing of three cranidia (Supplementary Data 5). The result of this analysis is that measurement error accounted for 4.84% of the total cranidial variance and thus was not a major contributor to the within-group or inter-group variance observed (see Supplementary Data 5). Bookstein (1991, p. 63–66) defined "type 1" landmarks when three surfaces intersect ("discrete juxtapositions of tissues") and "type 2" landmarks when two surfaces intersect ("maxima of curvature"), noting that arguments for positional homology are stronger for type 1 landmarks than for type 2. This study utilizes both these landmark types (Figs. 9, 12), but because *W. vanhornei* is somewhat effaced, the majority are type 2. Although we preferred to use type 1 landmarks where possible, measurement error in shape is broadly comparable to those of trilobites with a higher proportion of type 1 landmarks (e.g., Hong et al., 2014), a finding echoed by a recent comparative analysis among landmark categories (Wärmländer et al., 2019). The high proportion of type 2 landmarks used herein does not appear to have notably inflated observed variance.

Results

Cranidial shape changes.—The occipital-glabellar length of available *W. vanhornei* cranidia ranges from 1.40 mm to 4.30 mm, and across this span, analysis of cranidial shape change was based on 22 cranidial landmarks superimposed using general Procrustes superimposition of shape configurations of 17 cranidial specimens (Fig. 13).

A principal component analysis (PCA) of the partial warp scores (derived from the thin-plate spline analysis of Procrustes aligned landmarks based on the mean shape of the whole sample) shows that 68.44% of the shape variance is captured by the first three relative warps: Relative Warp 1 (RW 1), RW 2, and RW 3, respectively, explain 38.34%, 18.73%, and 11.37% of the total shape variance (Fig. 14.1). Each of the other 13 RWs accounts for less than 10.00% of the total variance, and they are not considered further (Supplementary Data 3). The deformation grids for the principal components were obtained by comparing minimum with maximum scores on each RW. RW 1 depicts an increase in relative length of the frontal area (sag.) and an overall contraction of the proportions of the glabella and of the eye (tr.) compared with other structures (Fig. 15.1). RW 2 depicts change in curvature of the frontal area, extension (sag.) of the L2 glabellar lobe, and contraction (sag.) of the L1 glabellar lobe (Fig. 15.2). RW 3 reflects widening of the fixigena (tr.) and of the frontal area (tr.) (Fig. 15.3). RW 1 and RW 2 display an interesting relationship in that specimens that score high on one axis score low on the other, and also show possible grouping (Fig. 14.1).

To investigate whether any of these patterns reflect ontogenetic change, the partial Procrustes distance of individual specimens from the mean of the smallest two cranidia specimens in the dataset was calculated and plotted against the natural log of centroid size as estimated by generalized Procrustes analysis (Fig. 16). A significant positive relationship exists between partial Procrustes distance and ln CCS (the natural log of centroid size, slope = 0.0486, p = 0.002267, r = 0.7241). Regression of partial warp scores from the mean shape of the smallest two cranidia specimens against ln CCS is significant (p = 0.003996 for 1,000 bootstraps) and suggests that 16.39% of overall shape variance captures ontogenetic variation. A deformation plot
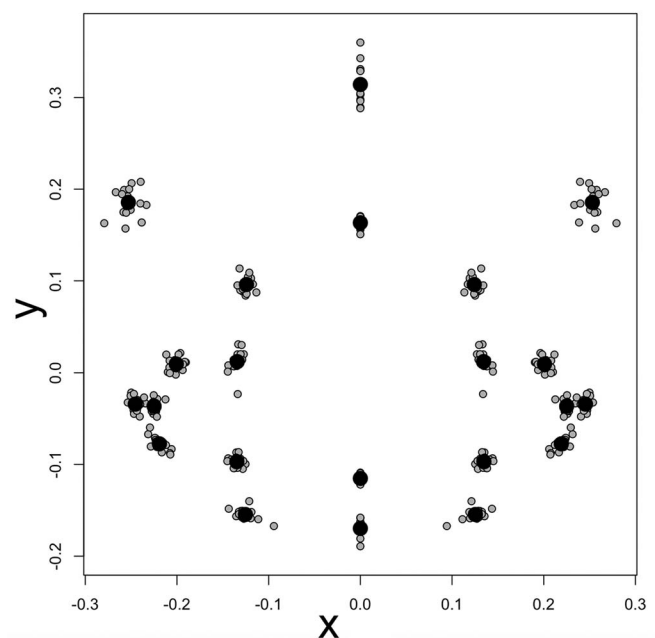
Figure 13. Procrustes superimposition of 22 landmarks for holaspid cranidia of *W. vanhornei,* (N = 17).
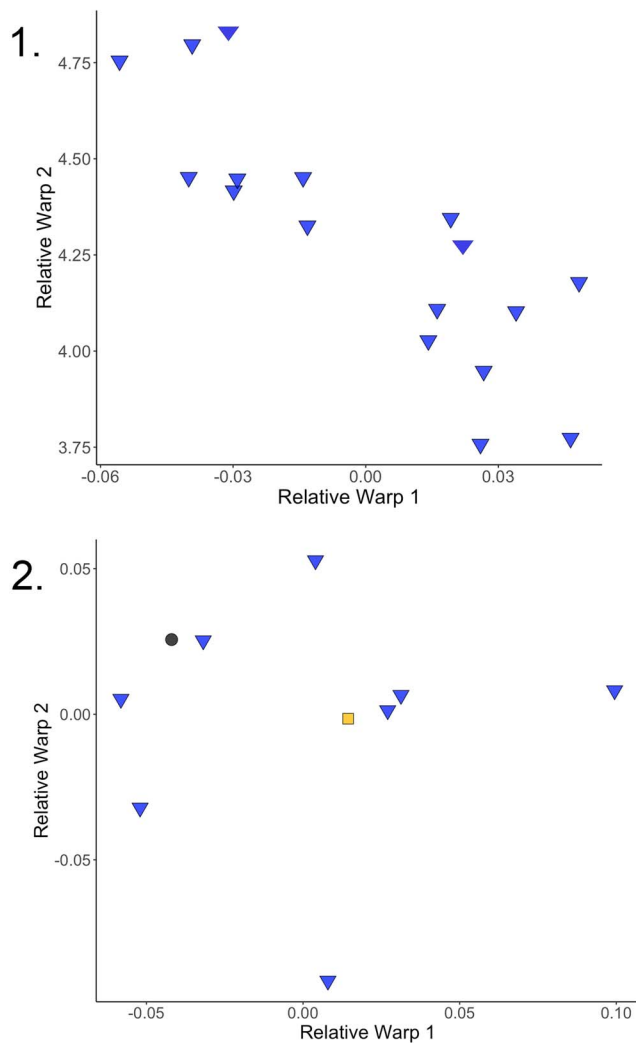
Figure 14. Bivariate scatter plots of first two principal components showing *Walcottaspis vanhornei* cranidia and pygidia categorized according to occurrence in the three localities. (**1**) Plot of principal components 1 and 2 for cranidial dataset showing 17 specimens from Hokah, Minnesota (blue inverted triangle). (**2**) Plot of principal components 1 and 2 for pygidial dataset showing eight specimens from Hokah, Minnesota (blue inverted triangle), one specimen from Winona, Minnesota (black circle), and one specimen from Bluff Siding, Wisconsin (yellow square).

was computed by regression of Procrustes aligned landmark data onto the ln CCS and using the predicted shapes from the regression model. Size-related shape change (Fig. 17) includes a relative decrease in frontal area length, particularly sagittally, accompanied by slight rearward migration of its widest point, slight negative allometry and abaxial migration of the palpebral lobe, and minor relative shortening of the occipital ring. According to sum squared calculation of predicted values from this regression, 28.64% of the cranidial shape variation is ontogenetic.

Pygidial shape variation.—The size range for the pygidium is from 2.00 mm to 5.50 mm in terms of total pygidial length (sag.).

We conducted three analyses of variation in pygidial shape for a total of 10 pygidia. One was a landmark-based analysis of

landmarks on the axis and pygidial margin that also included landmarks representing both the adaxial and abaxial extents of the pleural and interpleural furrows. The second was similar but also included semilandmarks interpolated along the course of each of these furrows. A third analysis was limited to the axial landmarks only. In all cases, the smallest well-preserved pygidium specimen was used as the sole ontogenetic reference in this analysis because its centroid size was far smaller than that of all other specimens such that the normal procedure of averaging several specimens to produce a small-sized reference form was not feasible. In no case did we find evidence of significant allometry among the pygidia, although this result may reflect the fact that only 10 specimens were part of the analysis. Nevertheless, the analysis did highlight notable patterns of morphological variation among these pygidia. Given no evident support for ontogeny-related variation, these can be summarized together. The main results are: (1) The principal morphological variation among pygidia is related to the proportions of the pygidial terminal piece, the length of the postaxial region, and the location of the widest point on the pygidium. Together, these summarize the proportion of the pygidium occupied by the axis. (2) Despite some arbitrariness in exact placement of the adaxial extents of pleural and interpleural furrows due to differential flattening, their positions and courses are notably stable among *W. vanhornei*, and especially so in the better-defined, more-anterior furrows. (3) In specimens in which the terminal piece is expanded, the third axial ring is notably contracted sagittally.

Pygidial shape variation based on 40 landmarks.—These include landmarks marking the abaxial and adaxial margins of six furrow left-right pairs in addition to the landmarks on the axis and pygidial margin (Fig. 12.1).

A PCA of the partial warp scores shows that 71.60% of the shape variance is captured by the first three relative warps: RW 1, RW 2, and RW 3, respectively, explain 32.15%, 21.14%, and 18.31% of the total shape variance (Fig. 14.2). Each of the other six principal components contains less than 15.00% of total variance (Supplementary Data 4). RW 1 captures mostly variation in the position of the abaxial extent of the last interpleural furrow, and this may be influenced by differential flattening but also suggests some variation in the ratio of axial to postaxial length (Fig. 18.1). Other than that, RW 1 also captures variation in the relative width of the axis. RW 2 shows variation in the proportions of the axial terminal piece with respect to the third axial ring and in the relative length of the postaxial field (Fig. 18.2). RW 3 shows variation in the position of pygidial maximum width and in the relative length of the postaxial field (Fig. 18.3).

The relationship between partial Procrustes distance and ln CCS is not significant (slope = 0.02274, p = 0.72000, r = 0.14170) (Fig. 19). Regression of partial warp scores against ln CCS is not significant at p = 0.3726 (at 1,000 bootstraps) but captures 12.23% of the total variance. Accordingly, while limitations of the sample preclude exclusion of any role for ontogeny in generating observed variance among holaspid *W. vanhornei* pygidia, its influence did not dominate observed variation.

Analysis of pygidial semilandmarks.—The traces of furrows on the pleural region of *Walcottaspis* pygidium invite investigation via semilandmarks (18 semilandmarks distributed along each of 6 left-right paired pleural furrows, Fig. 12.2).

Relative Warp 1

1.

2.

Relative Warp 2

3.
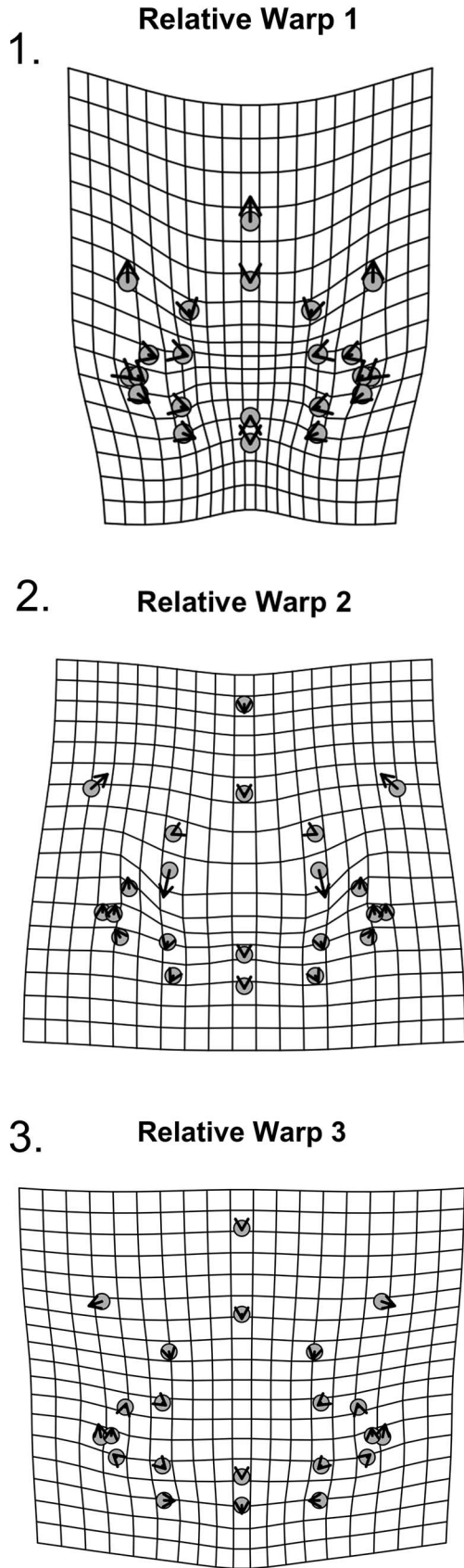
Relative Warp 3

Figure 15. Thin-plate spline deformation grid of relative warps for 22 landmarks for holaspid cranidia of *W. vanhornei* (N = 17). (**1**) Shape variation related to RW1. (**2**) Shape variation related to RW2. (**3**) Shape variation related to RW3.
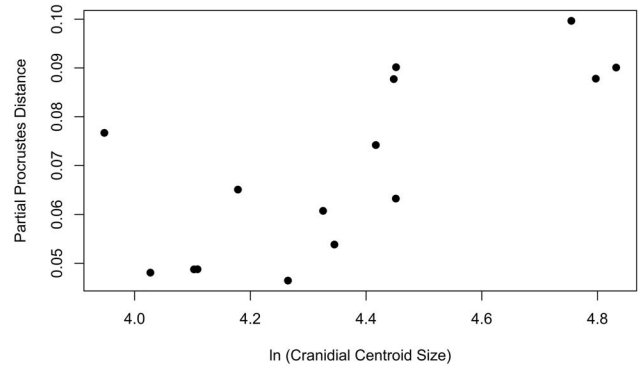
Figure 16. Partial Procrustes distance from the reference (mean shape of the smallest two cranidia) of 22 cranidial landmarks of *W. vanhornei* (N = 17).

The PCA of general Procrustes aligned landmarks shows that 75.36% of the shape variance is captured by the first three RWs. RW 1 depicts 37.83% of the shape variance in the form of expansion of the postaxial region and change in the extent of the posteriormost pleural furrows, which is likely influenced partly by degree of compaction (Fig. 20.1). RW 2 contains 22.76% of the shape variance and expresses minor variation in positions of the pleural and interpleural furrows (Fig. 20.2). RW 3 (14.77% of shape variance) depicts expansion of the postaxial region and contraction of the third axial ring (Fig. 20.3). Each of the six additional RWs contains less than 10.00% of the shape variance (Supplementary Data 4).

A nonsignificant negative relationship exists between partial Procrustes distance and ln CCS (slope = –0.02518, p = 0.2753, r = 0.4083) (Fig. 21). The regression of partial warp scores from the reference smallest specimen shape against ln CCS is also not significant (p = 0.4456 at 1,000 bootstraps).

Axial pygidial landmarks.—A subset of the previous data comprising 14 landmarks along the pygidial axis was chosen to explore variation therein (Fig. 12.3). The 10-specimen dataset was superimposed by generalized Procrustes analysis (Fig. 22).

The PCA of Procrustes aligned shape configurations shows that first two RWs capture almost the entire shape variance (84.38%): RW 1 captures more than half of the shape variance (54.61%,) and RW 2 explains 29.77% of the variance. Each of the remaining six RWs captures less than 15.00% of the shape variance in the dataset (Supplementary Data 4). RW 1 shows contraction of the length of the third axial segment while the posterior margin is extended and an overall contraction (tr.) of the axis is captured (Fig. 23.1). By contrast, RW 2 depicts expansion of the terminal axial piece, which decreases the relative length of the postaxial region (Fig. 23.2). The contraction of the third axial segment is consistently shown by both relative warps.

The relationship between partial Procrustes distance and ln CCS is not significant at p = 0.183 (slope = 0.2455, r = 0.488) (Fig. 24). When partial warp scores from the reference shape of the smallest specimen are regressed against ln CCS, the regression is not significant (p = 0.1598 at 1,000 bootstraps)

Overall, despite the low specimen abundance, *W. vanhornei* shows notable intraspecific variation in both the cranidium and pygidium, with most of this occurring in samples derived from
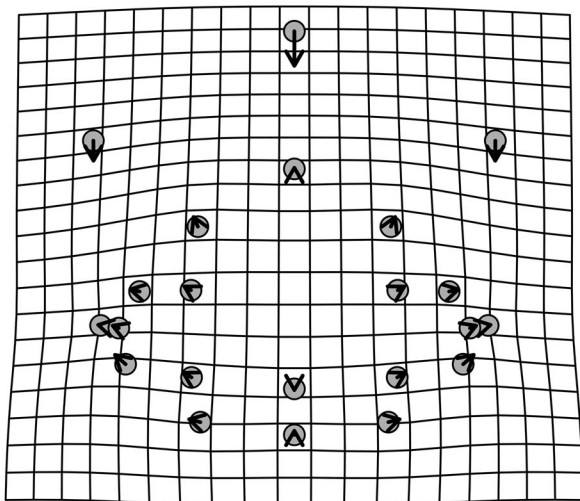
Figure 17. Thin-plate spline deformation grid of shape changes with growth for the 22 cranidial landmarks of *W. vanhornei* (N = 17).

a single locality, Hokah (HH), and there apparently from a single bed (Figs. 2, 14). The cranidium, known from more specimens, shows evident ontogenetic variation, something not confirmed for the pygidium. Pygidial morphological variation is nonetheless marked, particularly with respect to the length of the postaxial region, and again, this varies markedly within the collection made from the layer at about 6.6 m above the section base at Hokah (Fig. 14.2).

Materials

All specimens of *W. vanhornei* came from the heterolithic facies of the St. Lawrence Formation and are from Hokah, Minnesota, unless otherwise specified.

Repositories and institutional abbreviations.—Types, figures, and other specimens are reposited in the following institutions: University of Minnesota Paleontological Collection (UMPC, now part of the Cincinnati Museum Center [CMCIP] collection); Museum of Comparative Zoology, Harvard (MCZ); Field Museum of Natural History, Chicago (FMNH); University of Wisconsin, Madison (UWGM); United States National Museum of Natural History (USNM), and Yale Peabody Museum (YMP).

Systematic paleontology

In the following, we employ the synonymy list notations of Matthews (1973).

Class Trilobita Walch, 1773
Subclass Libristoma Fortey, 1990
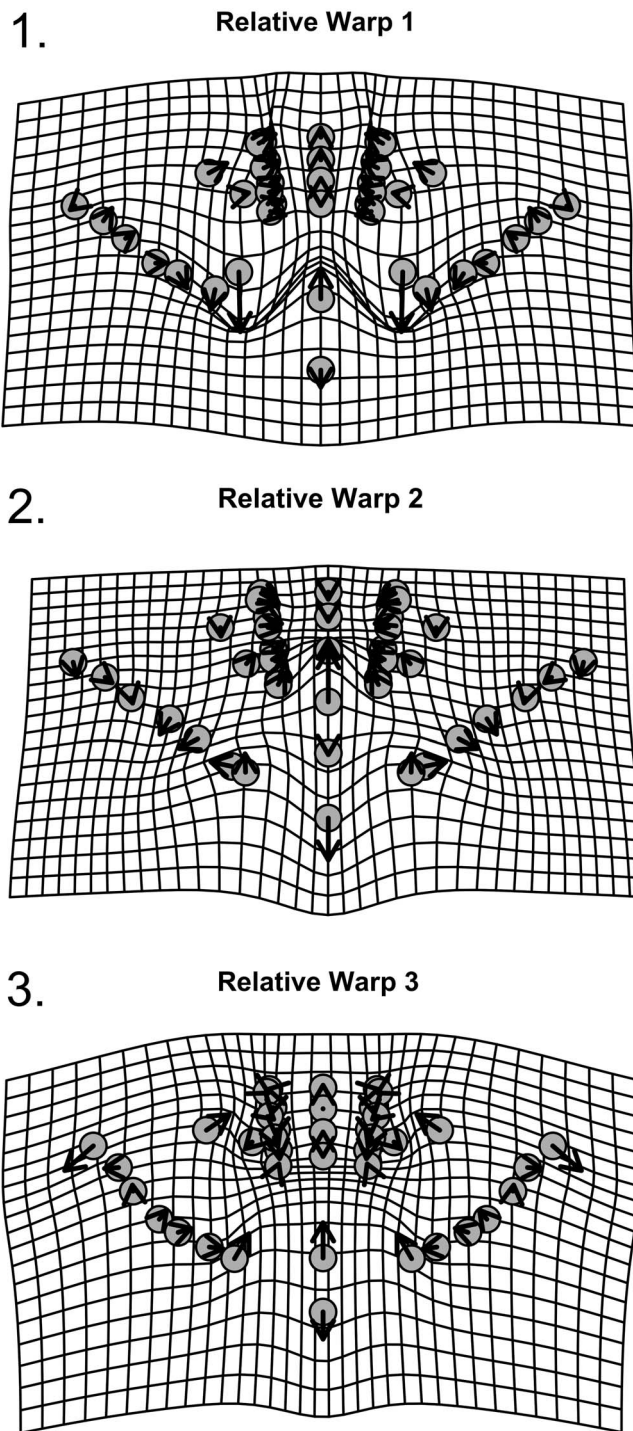
Figure 18. Thin-plate spline deformation grid of relative warps for 40 landmarks for pygidia of *W. vanhornei* (N = 10). (**1**) Shape variation related to RW1. (**2**) Shape variation related to RW2. (**3**) Shape variation related to RW3.

Order Asaphida Salter, 1864; emended Fortey, 1990
Superfamily Dikelocephalacea Miller, 1889 (emended Ludvigsen, Westrop, and Kindle, 1989)
Family Dikelocephalidae Miller, 1889; emended Ludvigsen, Westrop, and Kindle, 1989)
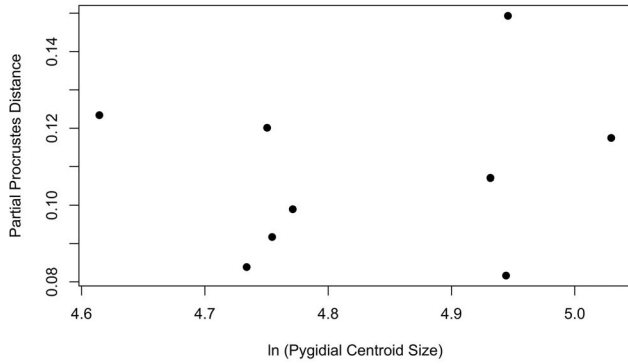
Figure 19. Partial Procrustes distance from the reference (mean shape of the smallest pygidium) of 40 pygidial landmarks of *W. vanhornei* (N = 10).

Remarks.—While the higher-level systematic relationship among members of this family and with its relatives will be discussed by us elsewhere, here we reject Ulrich and Resser's (1930) concept of Osceolinae because our phylogenetic analysis does not support a sister-taxon relationship between *W. vanhornei* and species of *Osceolia*. We consider *W. vanhornei* to be part of a clade containing those dikelocephalids with an extended cephalic doublure (see the preceding) and thus not part of the paraphyletic subfamily Dikelocephalinae as conceived of by Ludvigsen et al. (1989, p. 28), which contains taxa traditionally considered to be saukiid.

Genus *Walcottaspis* Ulrich and Resser, 1930

Type species.—*Walcottaspis vanhornei* (Walcott, 1914) from the heterolithic facies of the St. Lawrence Formation.

Diagnosis.—As for type species by monotypy.

Walcottaspis vanhornei (Walcott, 1914)
Figures 3, 5, 6

v*1914　*Dikelocephalus vanhornei* Walcott, p. 373, pl. 62, figs. 1–3.
v*1930　*Walcottaspis vanhornei* Ulrich and Resser, p. 65, pl. 20. figs. 3–5
1935　*Walcottaspis vanhornei* Twenhofel, Raasch, and Thwaites, p. 1712
1940　*Walcottaspis vanhornei* Richter and Richter, p. 24, pl. 25, fig. 4.
1951　*Walcottaspis vanhornei* Raasch, p. 141, 150.
1959　*Walcottaspis vanhornei* Lochman in Harrington et al., p. 254, fig. 191, 1a.
non v*1991　*Walcottaspis* sp. Shah et al., p. 91, pl. 1, figs. j, n.

Lectotype.—Selected herein: pygidium FMNH-UC14393-b from heterolithic facies of St. Lawrence Formation, Hokah (HH), Minnesota (Walcott, 1914, pl. 62, fig. 3).

Paralectotypes.—Cranidium (FMNH-UC14393-a) and thoracic segment (FMNH-UC14393-c) (Walcott, 1914, pl. 62, figs. 1, 2);
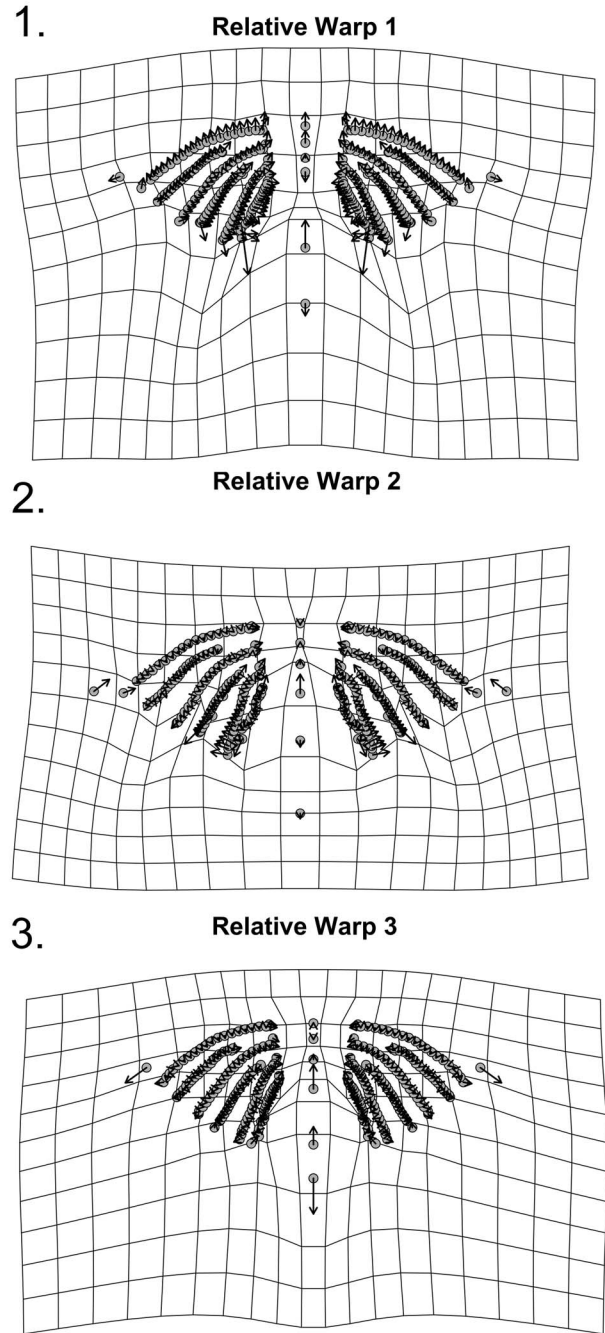
Figure 20. Thin-plate spline deformation grid of relative warps for 256 landmarks for pygidia of *W. vanhornei* (N = 10). (**1**) Shape variation related to RW1. (**2**) Shape variation related to RW2. (**3**) Shape variation related to RW3.

paralectotypes from the same bed as lectotype at Hokah (HH), Minnesota.

Diagnosis.—The S1 glabellar furrow isolated, transversely weakly incised, effaced in largest specimens. The S2 and additional glabellar furrows absent. Fixigena wide relative to other derived dikelocephalids. Pygidium with three clearly incised axial rings and long (sag.) terminal piece. Anterior pygidial margin fulcrate, transverse adaxially; posterior
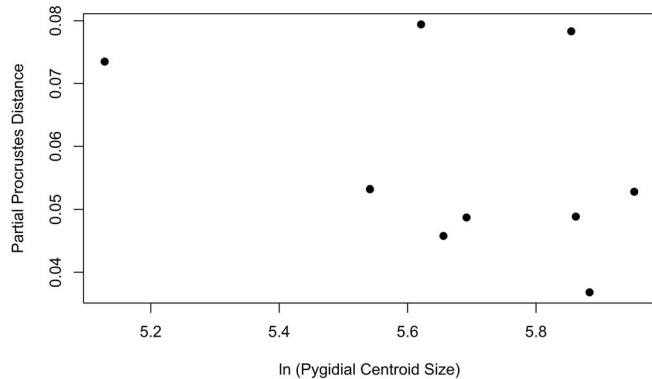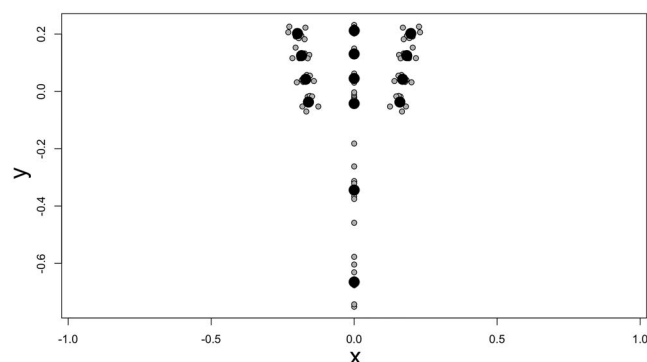
Figure 21. Partial Procrustes distance from the reference (mean shape of the smallest pygidium) of 256 pygidial landmarks of *W. vanhornei* (N = 10).

margin elliptical. Interpleural furrows of first two segments abruptly obsolete within pleural platform before approaching axial furrow. Postaxial region of variable length, but short (sag.).
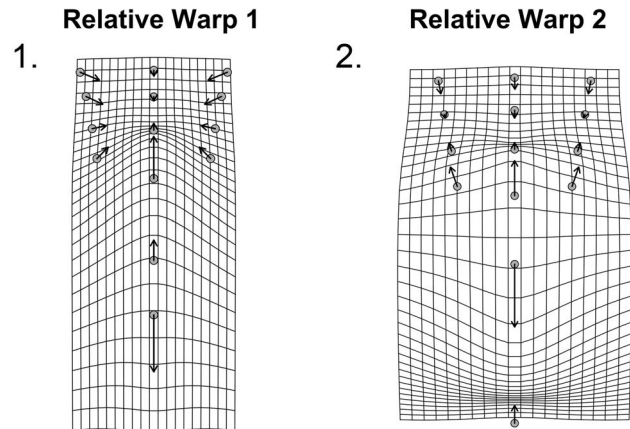
Occurrence.—*Eoconodontus* Zone, heterolithic facies of the St. Lawrence Formation within narrow outcrop belt including Hokah, Winona, and Reno, Minnesota, and Bluff Siding, Wisconsin.

Description.—Mature exoskeletons large, largest likely longer than 50 cm sagittally. Cephalon convex, outline semicircular, pygidium lateral margin shape matches that of anterior cephalon.

　　Glabella quadrate in smaller holaspids, trapezoidal in largest holaspids, inflated, maximum width just posterior to S1 furrow, expressed as slight bulge in L1. Glabellar anterior margin rounded. SO deepest adaxially, isolated in some specimens, shallowing transversely to yield slit-like furrow appearance. S1 isolated, variably incised but deepest axially where it forms an open U shape, running obliquely slightly forward abaxially. S2 obsolete. Median occipital tubercle present. Low, semicircular to transverse ridge shortly anterior to posterior margin of occipital ring. Axial furrow sharply incised. Frontal area long (sag.), broad (tr.), not less than 35% of occipital-glabellar length, flat to downsloping. The occipital lobe width is not less than 46% of the frontal area width. Anterior margin rounded to
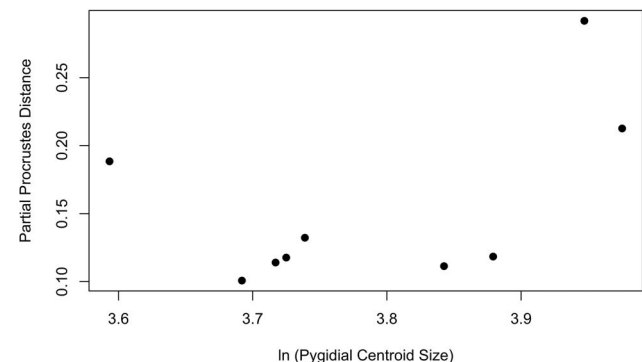

Figure 23. Thin-plate spline deformation grid of relative warps for 14 landmarks for pygidia of *W. vanhornei* (N = 10). (**1**) Shape variation related to RW1. (**2**) Shape variation related to RW2.

slightly angular axially, border absent. Frontal area width (tr) wider than maximum cranidial width between palpebral lobes (tr.) in smaller specimens, equal in larger. Opisthoparian dorsal cephalic suture marginal sagittally, laterally sweeps posteriorly at an angle of 20–41° to sagittal axis. Fixigenae wide for family, narrowest preocularly, shortly anterior to S1 where wider (tr.) than occipital lobe length (sag.). Intraocular fixed cheek inflated against palpebral furrow, sloping downward toward axial furrow (tr.). Palpebral lobes relatively short (exsag.) and narrow (tr.), midpoint opposite L1 bulge, relatively longer in smaller specimens. Palpebral furrow crescentic, deeply and evenly incised, eye ridge obsolete but ocular platform inflated to height of palpebral lobe distally. Posterior border area spatulate, terminating in blunt point abaxially, abaxial posterior portion with transverse ridge that parallels course of posterior border furrow. Posterior border furrow evenly incised, anterior face steeper than posterior, running transversely and posteriorly from point where SO projects to meet axial furrow.

　　Free cheeks arcuate, conjoined. Broad, undivided genal field, gently convex near the margin, rising steeply concavely toward flat ocular platform. Posterior border furrow sigmoidal,

Figure 22. Procrustes superimposition of 14 landmarks for pygidia including axis and posterior margin of *W. vanhornei* (N = 10).

Figure 24. Partial Procrustes distance from the reference (mean shape of the smallest pygidium) of 14 pygidial landmarks of *W. vanhornei* (N = 10).

curving posteriorly into base of narrow, long genal spine. Ocular incisure arcuate, bounded adaxially by shallow arcuate furrow and raised marginal flange forming eye socle. Terrace ridges on ocular platform inosculate. Doublure wide, extending about nine-tenths of distance from margin to ocular incisure, with flexure in its anterior portion that accommodates the anterior edge of hypostome. Doublure curves upward adaxially, remaining close beneath dorsal surface. Terrace ridges on doublure straight.

Hypostome subquadrangular, wider (tr.) than long (sag.); median body large, oval, inflated; anterior lobe convex, round; posterior lobe short (sag.), wide (tr.). Median furrow pit-like abaxially, shallow axially; maculae oval, small; pit-like furrows are developed at posterolateral margin of posterior lobe; border furrow weakly incised; lateral border triangular, widest (tr.) opposite midpoint of posterior lobe. Posterior border lip-like, gently arched anteriorly in axial portion. Terrace ridges on lateral border straight to sinuous, cuestaform, steep slopes facing adaxially.

Axial region of thoracic segments convex, articulating furrow transverse. Margins of thoracic pleurae transverse adaxially from axial furrow, curving posteriorly abaxial of fulcrum; anterior facet long (exsag.) abaxially of fulcrum; pleural furrow diagonal, firmly incised adaxially, reaching almost to tip of pleura; propleura and opisthopleura of equal length (exsag.) at fulcrum; pleural spine tip blunt. Fulcrum no more abaxial than one-third (tr.) of pleural width.

Pygidium anterior margin transverse adaxially, extending posterolaterally abaxial to fulcrum; posterior margin entire, semielliptical. Axis convex, 60–72% of pygidial length (sag.) with anterior articulating half-ring, three distinct axial rings defined by narrow and well-incised inter-ring furrows, long (sag.) terminal piece. Ridge arches anteriorly from posterior border of first axial ring, occupying medial three-quarters of ring width (tr.) and extending across one-half of ring length (sag.) Each axial ring with pair of swollen nodes located anterior of segment midline (exsag.) near axial furrow; two additional pairs of the lobes extend onto terminal piece in lectotype, which also shows one additional incomplete rachial furrow. Terminal piece may be inflated, posterior margin blunt, rounded to bullet-shaped. Pleural furrows entire, extending to near margin in anterior segments; interpleural furrows of first two segments abruptly obsolete on pleural platform approaching axial furrow; third interpleural furrow connects to axis at posterior of third axial ring. Postaxial region short (sag.) but of variable length. Petaloid terraces developed on articulating facet of first pleura. Doublure extends to pleural platform lying close beneath dorsal surface, with faint paradoublural line, terrace ridges on it straight, relief high, steeper slopes facing outward; some 25 terraces from top of pleural platform to margin.

Other material.—All from Hokah, Minnesota, unless otherwise stated. Twenty-one cranidia (FMNH-PE-39216-c, FMNH-PE-39214, FMNH-PE-39215, FMNH-UC-23314-a, FMNH-UC-23314-b, FMNH-UC-23314-c, FMNH-UC-23314-d, CMC-IP-87565x, CMC-IP-89411h, CMC-IP-89411i, CMC-IP-87565j, CMC-IP-89411m, CMC-IP-87565n, CMC-IP-87565t, CMC-IP-95630, UWGM 7150, UWGM 7151, UWGM 7152, UWGM 7155, UWGM 7156, YMP73152), 19 pygidia (FMNH-PE-39216-a, FMNH-PE-39216-b, FMNH-

PE-39210, FMNH-PE-39312, FMNH-UC-23314-e, FMNH-UC-14393-b, MCZ-IP910 from Bluff Siding, Wisconsin, CMC-IP-89411a, CMC-IP-89411b, CMC-IP-89411c, CMC-IP-87565d, CMC-IP97568, USNM-PAL-72687A from Winona, Minnesota, USNM-PAL-72687B from Winona, Minnesota, UWGM 7157, UWGM 7158, UWGM 7159, UWGM 7160, UWGM 7161), five disarticulated free-cheek specimens (FMNH-UC-23314-h2, FMNH-UC-23314-h, FMNH-UC-23314-h1, FMNH-UC-23314-i, CMC-IP89411y), three hypostomes (FMNH-UC-23314-f, FMNH-UC-23314-f, FMNH-UC-23314-g), one conjoined free cheek (MCZ-IP-917 from Bluff Siding, Wisconsin), and two thoracic segment specimens (FMNH-PE-82162, FMNH-UC-14393-c). Other previously figured material includes one pygidium (USNM-PAL-72687A) from Winona, Minnesota (Ulrich and Resser, 1930, pl. 20, fig. 6; Fig. 5.4) and one plastotype cranidium (USNM-PAL 58608-a) and one plastotype pygidium (USNM-PAL 58608-b) cast from Walcott's (1914) figured specimens (FMNH-UC-14393-a and FMNH-UC-14393-b; Ulrich and Resser, 1930, pl. 20, figs. 3, 4).

Remarks.—The proportions of the posterior trunk in our reconstruction are based on a pygidial size in which the marginal outline best matches the shape of the anterior cephalic doublure, which it does closely and that may also suggest spheroidal enrollment in this trilobite. Proportioning the pygidium in this way and assuming 12 thoracic segments in maturity, as known in *D. minnesotensis*, yields an overall body plan that seems realistic (Fig. 6.2). However, the number of thoracic segments in holaspid *W. vanhornei* is unknown. Given that *W. vanhornei* has one fewer clearly defined holaspid pygidial segment than *D. minnesotensis,* one possibility is that the total number of trunk segments was common to both species and that the evolution of *W. vanhornei* from a *minnesotensis*-like ancestor reflected release of the leading pygidial segment into the mature thorax (see Hughes, 1994, p. 53). If the pygidial spines in *D. minnesotensis* were related to this leading segment, then the striking morphological difference between their pygidia might be explained without invoking major body repatterning because the two species may have had quite similar trunk forms, their principal difference being where the pygidial boundary was situated. Although this suggestion is speculative, it illustrates how the trilobite trunk region, with its variations not only in the form and degree of integration between segments but also in their overall number and allocation to the mature thorax or pygidium, offered more "degrees of freedom" to vary than the cephalon and may explain, in part, why the cranidia of *W. vanhornei* and *D. minnesotensis* remain much more similar than their pygidia. However, in the posterior of the thorax of *D. minnesotensis*, segments lost the fulcrum and became markedly more siculate, whereas in *W. vanhornei*, the fulcrum was maintained throughout the trunk as it is present in both the holaspid posterior cephalic and anterior pygidial margins. This suggests a lower gradient of thoracic segment shape change in *W. vanhornei* than in *D. minnesotensis.* A number of determinants of trunk structure were evidently adjusted during the evolution of *W. vanhornei*.

Walcott's (1914, pl. 62, fig. 3) illustration of the lectotype pygidium of *W. vanhornei* was "retouched," an ink-based outlining technique used at will to emphasize subtle features. His figure suggests that the terminal piece bears possibly as many as four transverse furrows in addition to those defining the three clear axial segments. These additional furrows are not visible in the image of the same specimen provided by Ulrich and Resser (1930, pl. 20, fig. 4), but our illustrations (Figs. 4.1, 5.7) confirm some transverse structures within the terminal piece. Recognition of an incompletely expressed fourth segment is warranted on the basis of the nodes and furrow expressed, and there may be a fifth set of nodes, but we do not see evidence for all the four additional segments that Walcott (1914, fig. 3) depicted. Furthermore, furrows expressed in the pleural region relate only to the first three axial segments. Such imprecision in segment counts is not surprising. The terminal piece housed the zone of teloblastic cells from which new segments derived, and trilobites varied in the ways in which new trunk segments were expressed with, for example, mismatches known between the numbers of ventral appendages and segments expressed in the exoskeleton (Hughes, 2003). However, there is no evidence of a change in the number of well-expressed segments during the part of the holaspid ontogeny of *W. vanhornei* available for analysis: it is three in all specimens, as opposed to the four segments clearly expressed in both axis and pleural region in most *D. minnesotensis*, a species that also has additional, indistinctly expressed segments in its terminal piece. Accordingly, we consider the two species to differ in the number of firmly expressed pygidial segments and this difference between them to be not simply variation in the prominence with which the most posterior segments are expressed.

The distinctive elliptical pygidial shape of *W. vanhornei* is homeomorphic with that of several other trilobites. Examples from the same region include *Briscoia pertransversa* Lochman (1956) from the *Prosaukia* Zone of the Tunnel City Group and likewise *Wilbernia* sp. occurring in the "Hudson Member" of the Lone Rock Formation in lower stratigraphic units (Fig. 10). Both these other examples also bear three clearly expressed segments in the axis and matching pleural and interpleural furrows that mimic those of the thorax (i.e., all trunk segments are homonomous in structure; Hughes, 2003). Such pygidia must link articulating thoracic segments to the terminal piece across a short interval of three pygidial segments. If the postaxial region is short, then an elliptical shape for the pygidial posterior shape is required to produce the necessary pleural width at the anterior of the pygidium to allow integration with the thorax. Accordingly, it is not unexpected that pygidial shape and furrow structure arose iteratively in various groups at that time. However, *W. vanhornei* is clearly distinguished from such homeomorphs by its unique termination of the anterior interpleural furrows and by the features that place it as sister taxon to *D. minnesotensis,* which bore a more segment-rich pygidium.

Acknowledgments

Declaration of competing interests

The authors declare none.

Data availability statement

Data available from the Dryad Digital Repository: https://doi.org/10.5061/dryad.h70rxwdpd.

References

Adams, D.C., Collyer, M.L., Kaliontzopoulou, A., and Baken, E.K., 2021, Geomorph: Software for geometric morphometric analyses. R package version 4.0. https://cran.r-project.org/package=geomorph (accessed Jul 2022).

Anderson, M., and Braak, C.T., 2003, Permutation tests for multi-factorial analysis of variance: Journal of Statistical Computation and Simulation, v. 73, p. 85–113, https://doi.org/10.1080/00949650215733.

Baken, E.K., Collyer, M.L., Kaliontzopoulou, A., and Adams, D.C., 2021, gmShiny and geomorph v.4.0: new graphical interface and enhanced analytics for a comprehensive morphometric experience: Methods in Ecology and Evolution, v. 12, p. 2355–2363, https://doi.org/10.1111/2041-210X.13723.

Beheregaray, L.B., and Sunnucks, P., 2001, Fine-scale genetic structure, estuarine colonization and incipient speciation in the marine silverside fish *Odontesthes argentinensis*: Molecular Ecology, v. 10, p. 2849–2866, https://doi.org/10.1046/j.1365-294X.2001.t01-1-01406.x.

Bell, W.C., Feniak, O.W., and Kurtz, V.E., 1952, Trilobites from the Franconia Formation, Southeast Minnesota: Journal of Paleontology, v. 26, p. 175–198.

Bell, W.C., Berg, R.R., and Nelson, C.A., 1956, Croixan type area–Upper Mississippi Valley, *in* Rodgers, J., ed., El Sistema Cambrico, su Paleogeografia y el problema de su Base, Tomo II, Parte II: Australia, America, Mexico, XX Congreso Geological Internacional, p. 415–446.

Bookstein, F.L., 1991, Morphometric tools for landmark data: New York, Cambridge University Press, 435 p.

Bremer, K., 1988, The limits of amino acid sequence data in angiosperm phylogenetic reconstruction: Evolution, v. 42, p. 795–803, https://doi.org/10.1111/j.1558-5646.1988.tb02497.x.

Bremer, K., 1994, Branch support and tree stability: Cladistics, v. 10, p. 295–304, https://doi.org/10.1111/j.1096-0031.1994.tb00179.x.

Collyer, M.L., and Adams, D.C., 2018, RRPP: An R package for fitting linear models to high-dimensional data using residual randomization: Methods in Ecology and Evolution, v. 9, p. 1772–1779, https://doi.org/10.1111/2041-210X.13029.

Collyer, M.L., and Adams, D.C., 2021, RRPP: Linear Model Evaluation with Randomized Residuals in a Permutation Procedure. https://cran.r-project.org/web/packages/RRPP (accessed Jul 2022).

Dolby, G.A., Ellingson, R.A., Findlay, L.T., and Jacobs, D.K., 2018, How sea level change mediates genetic divergence in coastal species across regions with varying tectonic and sediment processes: Molecular Ecology, v. 27, p. 994–1011, https://doi.org/10.1111/mec.14487.

Fortey, R.A., 1990, Ontogeny, hypostome attachment and trilobite classification: Palaeontology, v. 33, p. 529–576.

Goloboff, P.A., Farris, J.S., and Nixon, K.C., 2008, TNT, a free program for phylogenetic analysis: Cladistics, v. 24, p. 774–786, https://doi.org/10.1111/j.1096-0031.2008.00217.x.

Grunstra, N.D.S., Bartsch, S.J., Le Maître, A., and Mitteroecker, P., 2021, Detecting phylogenetic signal and adaptation in *Papionin* cranial shape by decomposing variation at different spatial scales: Systematic Biology, v. 70, p. 694–706, https://doi.org/10.1093/sysbio/syaa093.

Hall, J., 1863, Preliminary Notice of the Fauna of the Potsdam Sandstone: Sixteenth Annual Report of the Regents of the University of the State of New York on the Condition of the State Cabinet of Natural History, p. 119–226.

Harrington, H.J., Henningsmoen, G., Howell, B.F., Jaanuson, V., Lochman-Balk, C., et al., 1959, Trilobita, *in* Moore, R.C., ed., Treatise on Invertebrate Paleontology, Part O, Arthropoda, Volume 1: Lawrence, Kansas, Geological Society of America and University of Kansas Press, p. O38–O560.

Hong, P.S., Hughes N.C., and Sheets, H.D.C., 2014, Size, shape and systematics of the Silurian trilobite *Aulacopleura koninckii:* Journal of Paleontology, v. 88, p. 1120–1138.

Hughes, N.C., 1993, Distribution, taphonomy and functional morphology of the upper Cambrian trilobite *Dikelocephalus*: Milwaukee Public Museum Contributions in Biology and Geology, v. 84, 49 p.

Hughes, N.C., 1994, Ontogeny, intraspecific variation, and systematics of the late Cambrian trilobite *Dikelocephalus*: Smithsonian Contributions to Paleobiology, v. 79, 89 p., https://doi.org/10.5479/si.00810266.79.1.

Hughes, N.C., 1999, Statistical and imaging methods applied to deformed fossils, *in* Harper, D.A.T., ed., Numerical Palaeobiology: London, John Wiley, p. 127–155.

Hughes, N.C., 2003, Trilobite tagmosis and body patterning from morphological and developmental perspectives: Integrative and Comparative Biology, v. 41, p. 185–206, https://doi.org/10.1093/icb/43.1.185.

Hughes, N.C., and Hesselbo, S.P., 1997, Stratigraphy and sedimentology of the St. Lawrence Formation, upper Cambrian of the northern Mississippi Valley: Milwaukee Public Museum Contributions in Biology and Geology, v. 91, 50 p.

Hughes, N.C., Adrain, J.M., Holmes, J.D., Hong, P.S., Hopkins, M.J., et al., 2021, Articulated trilobite ontogeny: suggestions for a methodological standard: Journal of Paleontology, v. 95, p. 298–304, https://doi.org/10.1017/jpa.2020.96.

Jablonski, D., and Bottjer, D.J., 1990, The ecology of evolutionary innovation: the fossil record, *in* Nikecki, M.H., ed., Evolutionary Innovations: Chicago, University of Chicago Press, p. 253–288.

Jablonski, D., Sepkoski, J.J. Jr., Bottjer, D.J., and Sheehan, P.M., 1983, Onshore–offshore patterns in the evolution of Phanerozoic shelf communities: Science, v. 222, p. 1123–1125, https://doi.org/10.1126/science.222.4628.1123.

Jacobs, D.K., and Lindberg, D.R., 1998, Oxygen and evolutionary patterns in the sea: onshore–offshore trends and recent recruitment of deep-sea faunas: Proceedings of the National Academy of Sciences of the United States of America, v. 95, p. 9396–9401, https://doi.org/10.1073/pnas.95.16.9396.

Jell, P.A., and Hughes, N.C., 1997, Himalayan Cambrian trilobites: Special Papers in Palaeontology, v. 58, 113 p.

Kobayashi, T., 1935, The *Briscoia* fauna of the late upper Cambrian in Alaska with descriptions of a few upper Cambrian trilobites from Montana and Nevada: Japanese Journal of Geology and Geography, v. 12, p. 39–57.

Kobayashi, T., 1942, Two new trilobite genera, *Hamashania* and *Kirkella*: Journal of the Geological Society of Japan, v. 59, p. 37–40.

Kowalewski, M., and Bambach, R.K., 2003, The limits of paleontological resolution, *in* Harries, P.J., ed., High Resolution Approaches in Stratigraphic Paleontology: Dordrecht, Kluwer Academic Publishers, p. 1–48.

Lochman, C., 1956, The evolution of some upper Cambrian and Lower Ordovician trilobite families: Journal of Paleontology, v. 30, p. 445–462, http://www.jstor.org/stable/1300283.

Ludvigsen, R., Westrop, S.R., and Kindle, C.H., 1989, Sunwaptan (upper Cambrian) trilobites of the Cow Head Group, western Newfoundland, Canada: Palaeontographica Canadiana, v. 6, 175 p.

Luo, H.-L., Hu, S.-X., Hou, S.-G., Gao, H.-G., Zhan, D.-Q., and Li, W.-C., 2009, Cambrian stratigraphy and trilobites from southeastern Yunnan, China: Kunming, Yunnan Science and Technology Press, 252, p.

Matthews, S.C., 1973. Notes on open nomenclature and on synonymy lists: Palaeontology, v. 16, p. 713–719.

Miller, J.F., 1969, Conodont fauna of the Notch Peak Limestone (Cambro-Ordovician), House Range, Utah: Journal of Paleontology, v. 43, p. 413–439.

Miller, J.F., Evans, K.R., Loch, J.D., Ethington, R.L., Stitt, J.H., Holmer, L., and Popov, L.E., 2003, Stratigraphy of the Sauk III interval (Cambrian–Ordovician) in the Ibex area, western Millard County, Utah and Central Texas: Brigham Young University Geology Studies, v. 47, p. 23–118 (plus CD-ROM with 17 section descriptions and 23 tables).

Miller, S.A., 1889, North American Geology and Palaeontology for the Use of Amateurs, Students, and Scientists: Cincinnati, Western Methodist Book Concern, 664 p.

Mitteroecker, P., Bartsch, S., Erkinger, C., Grunstra, N.D.S., Le Maître, A., and Bookstein, F.L., 2020, Morphometric variation at different spatial scales: coordination and compensation in the emergence of organismal form: Systematic Biology, v. 69, p. 913–926, https://doi.org/10.1093/sysbio/syaa007.

Mossler, J.H., 1992, Sedimentary rocks of Dresbachian age (late Cambrian), Hollandale embayment, southeastern Minnesota: University of Minnesota Report of Investigations, v. 40, 71 p., https://hdl.handle.net/11299/60785.

Myrow, P.M., Taylor, J.F., Miller, J.F., Ethington, R., Ripperdan, R.L., and Allen, J., 2003, Fallen arches: dispelling myths concerning Cambrian and Ordovician paleogeography of the Rocky Mountain region: Geological Society of America Bulletin, v. 115, p. 695–713, https://doi.org/10.1130/0016-7606(2003)115<0695:FADMCC>2.0.CO;2.

Nelson, C.A., 1956, Upper Croixan stratigraphy, upper Mississippi Valley: Geological Society of America Bulletin, v. 67, p. 165–184, https://doi.org/10.1130/0016-7606(1956)68[165:UCSUMV]2.0.CO;2.

Nixon, K.C., 1999–2002, WinClada, v. 1.0000: Ithaca, New York, published by the author.

Olszewski, T., 1999, Taking advantage of time averaging: Paleobiology, v. 25, p. 226–238, https://doi.org/10.1017/S009483730002652X.

Owen, D.D., 1852, Report of a Geological Survey of Wisconsin, Iowa, and Minnesota: Philadelphia, Lippincott, Grambo and Company, 638 p.

Palmer, A.R., 1960, Some aspects of the early upper Cambrian stratigraphy of White Pine County, Nevada and vicinity, *in* Boettcher, J.W. Jr. and Sloan, W.W., eds., Guidebook to the Geology of East Central Nevada, Eleventh Annual Field Conference: Intermountain Association of Petroleum Geologists, p. 53–58.

Paola, C., Ganti, V., Mohrig, D., Runkel, A.C., and Straub, K.M., 2018, Time not our time: physical controls on the preservation and measurement of geologic time: Annual Reviews of Earth and Planetary Sciences, v. 46, p. 409–438, https://doi.org/10.1146/annurev-earth-082517-010129.

Raasch, G.O., 1939, Cambrian Merostomata: Geological Society of America Special Papers, v. 19, 146 p.

Raasch, G.O., 1951, Revision of the Croixan dikelocephalids: Transactions of the Illinois Academy of Science, v. 44, p. 137–151.

Resser, C.E., 1937, Third contribution to the nomenclature of Cambrian fossils: Smithson Miscellaneous Collections, v. 95, p. 1–29.

Richter, R., and Richter, E., 1940, Die *Saukianda*-Stufe von Andalusien, eine frende Fauna im europäischen Ober-Kambrium: Abhandungrn der Senkenbergischen Naturforschenden Gesellschaft, v. 450, 88 p. [in German]

Runkel, A.C., 1994, Deposition of the uppermost Cambrian (Croixan) Jordan sandstone, and the nature of the Cambrian–Ordovician boundary in the Upper Mississippi Valley: Geological Society of America Bulletin, v. 106, p. 492–506.

Runkel, A.C., Miller, J.F., McKay, R.M., Palmer, A.R., and Taylor, J.F., 2007, High-resolution sequence stratigraphy of lower Paleozoic sheet sandstones in central North America: the role of special conditions of cratonic interiors in development of stratal architecture: Geological Society of America Bulletin, v. 119, p. 860–881, https://doi.org/10.1130/B26117.1.

Salter, J.W., 1864, A monograph of British trilobites: Monographs of the Palaeontographical Society, v. 16, no. 67, 83 p., https://doi.org/10.1080/02693445.1864.12113212.

Sepkoski, J.J. Jr., 1991, A model of onshore–offshore change in faunal diversity: Paleobiology, v. 17, p. 58–77, https://doi.org/10.1017/S0094837300010356.

Shah, S.K., Parcha, S.K., and Raina, A.K., 1991, Late Cambrian trilobites from Himalaya: Journal of the Palaeontological Society of India, v. 36, p. 89–107.

Shen, K.-N., Jamandre, B.W., Hsu, C.-C., Tzeng, W.-T., and Durand, J.-D., 2011, Plio-Pleistocene sea level and temperature fluctuations in the northwestern Pacific promoted speciation in the globally-distributed flathead mullet *Mugilcephalus*: BMC Evolutionary Biology, v. 11, n. 83, https://doi.org/10.1186/1471-2148-11-83.

Twenhofel, W.H., Raasch, G.O., and Thwaites, F.T., 1935, Cambrian strata of Wisconsin: Geological Society of America Bulletin, v. 46, p. 1687–1744, https://doi.org/10.1130/GSAB-46-1687.

Ulrich, E.O., and Resser, C.E., 1930, The Cambrian of the Upper Mississippi Valley, Part 1: Trilobita; Dikelocephalinae and Osceolinae: Bulletin of the Public Museum, Milwaukee, v. 12, 122 p.

Walch, J.E.I., 1773, De natuurlyke Historie der Versteeningen of uitvoerige Afbeelding en Beschryving van de Versteende Zaaken, die tot heden op den Aardbodem zyn ontdekt: Amsterdam, Jan Christian Sepp, 303 p.

Walcott, C.D., 1879, Description of new species of fossils from the Calciferous Formation: New York State Museum, 31st Annual Report, p. 129–131.

Walcott, C.D., 1884, Paleontology of the Eureka district: Monographs of United States Geological Survey, v. 8, 285 p.

Walcott, C.D., 1914, Cambrian geology and paleontology II: *Dikelocephalus* and other genera of the Dikelocephalinae: Smithsonian Miscellaneous Collections, v. 57, p. 345–430.

Walcott, C.D., 1924, Cambrian and lower Ozarkian trilobites: Smithsonian Miscellaneous Collections, v. 75, p. 55–60.

Wärmländer, S.K.T.S., Garvin, H., Guyomarc'h, P., Petaros, A., and Sholts, S.B., 2019, Landmark typology in applied morphometric studies: what's the point?: The Anatomical Record, v. 302, p. 1144–1153, https://doi.org/10.1002/ar.24005.

Westrop, S.R., 1986, Trilobites of the upper Cambrian Sunwaptan Stage, southern Canadian Rocky Mountains, Alberta: Palaeontographica Canadiana, v. 3, 179 p.

Winston, D., and Nicholls, H., 1967, Late Cambrian and Early Ordovician faunas from the Wilberns Formation of Central Texas: Journal of Paleontology, v. 41, p. 66–96.

Zhang, W.-T., Lu, Y.-H., Chu, C.-L., Qian, Y.-Y., Lin, H.-J., Zhou, Z.-Y., Zhang, S.-G., and Yuan, J.-L., 1980, Cambrian trilobite faunas of southwestern China: Palaeontologia Sinica New Series B, v. 16, 497 p.